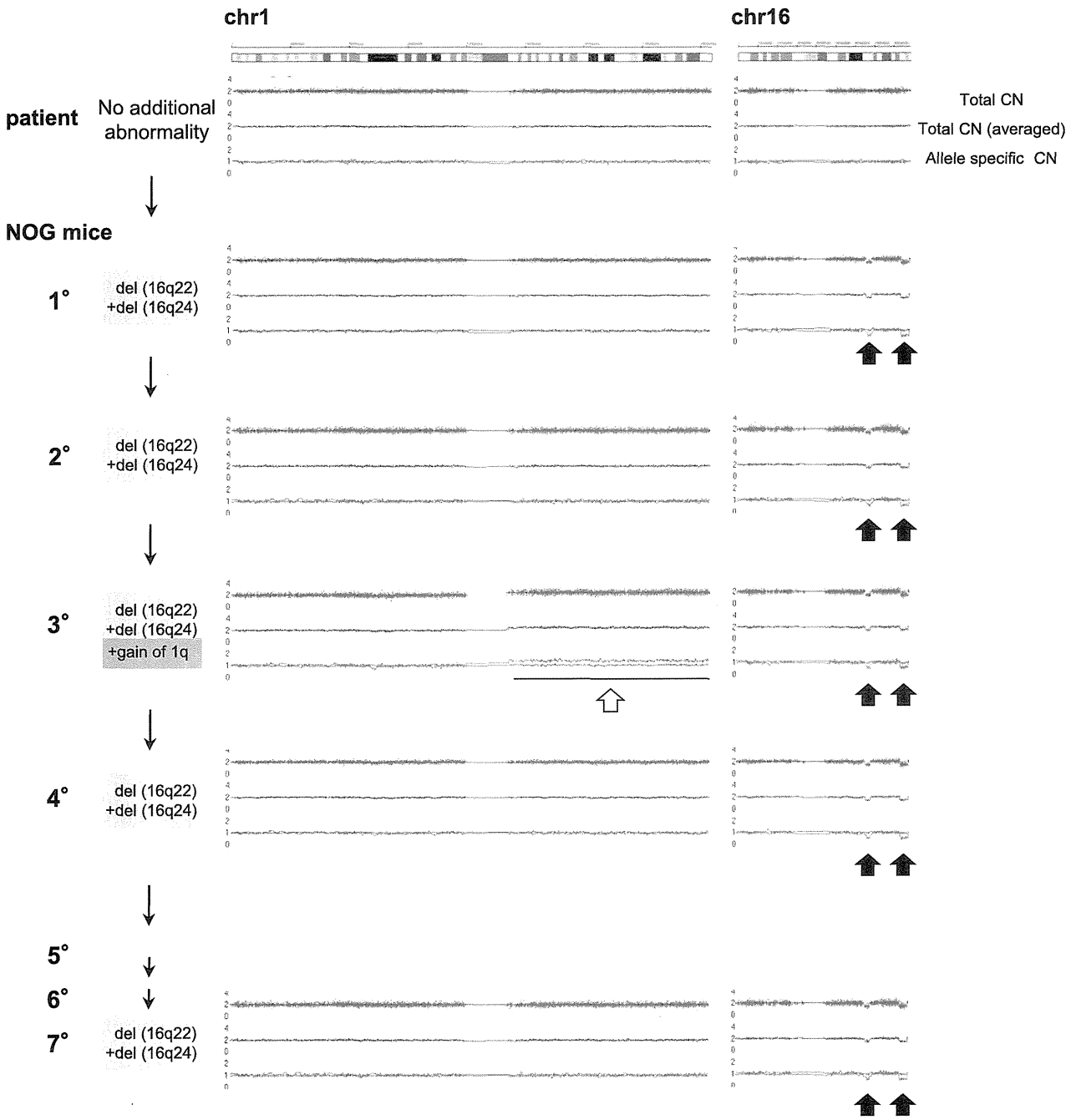

Figure 3. Sequential CNA analysis of TAM-derived cells in the recipients of patient 1. DNA obtained from the original patient sample and sorted hCD45$^+$ recipient BM cells were analyzed by Affymetrix GeneChip Mapping 250K arrays and compared with the PB sample of the original patient in complete remission phase. The primary sample of the patient in TAM phase (blast 92%) had no CNA. hCD45$^+$ BM cells of 1° to 7° recipients had a hemi-allelic deletion in regions 16q22 and 16q24 (black arrows). The 3° recipient had a gain of the entire arm of chromosome 1q (white arrow) in addition to deletion of 16q22 and 16q24. Arrowhead indicates abnormal CNA.

(Figure 4A). To determine whether these subclones were present at low levels in the primary sample of patient 1, specific PCR for the 16q22 deletion was performed using primer pairs designed to bookend the deletion site. CNA analysis and genome sequencing data in these deletion sites (16q22 and 16q24) revealed the presence of genomic breakage and inversion (Figure 5A; supplemental Figures 3 and 4; see supplemental Methods for details). A primer set was designed to detect the deduced breakpoint and used to perform PCR on TAM-derived cells from patient 1 in the recipients with 16q22 and 16q24 deletions. PCR using genomic DNA from TAM-derived cells in the 1° to 8° recipients of the first series of transplantations (Figure 3) produced a uniformly bright DNA fragment of the same size, consistent with the results of CNA profiling (Figure 5B). A faint fragment was detected by applying this PCR method to genomic DNA from the primary patient sample (patient 1), which was confirmed to contain the deletion breakpoint in 16q22 by Sanger sequencing. These results demonstrated that TAM cells with the 16q22 and 16q24 deletions already resided as a minor population in the original sample of patient 1. The frequency of the mutant cells was estimated to be ~1.0% to 0.2% of the patient's PBMCs by a serial dilution assay (supplemental Figure 5).

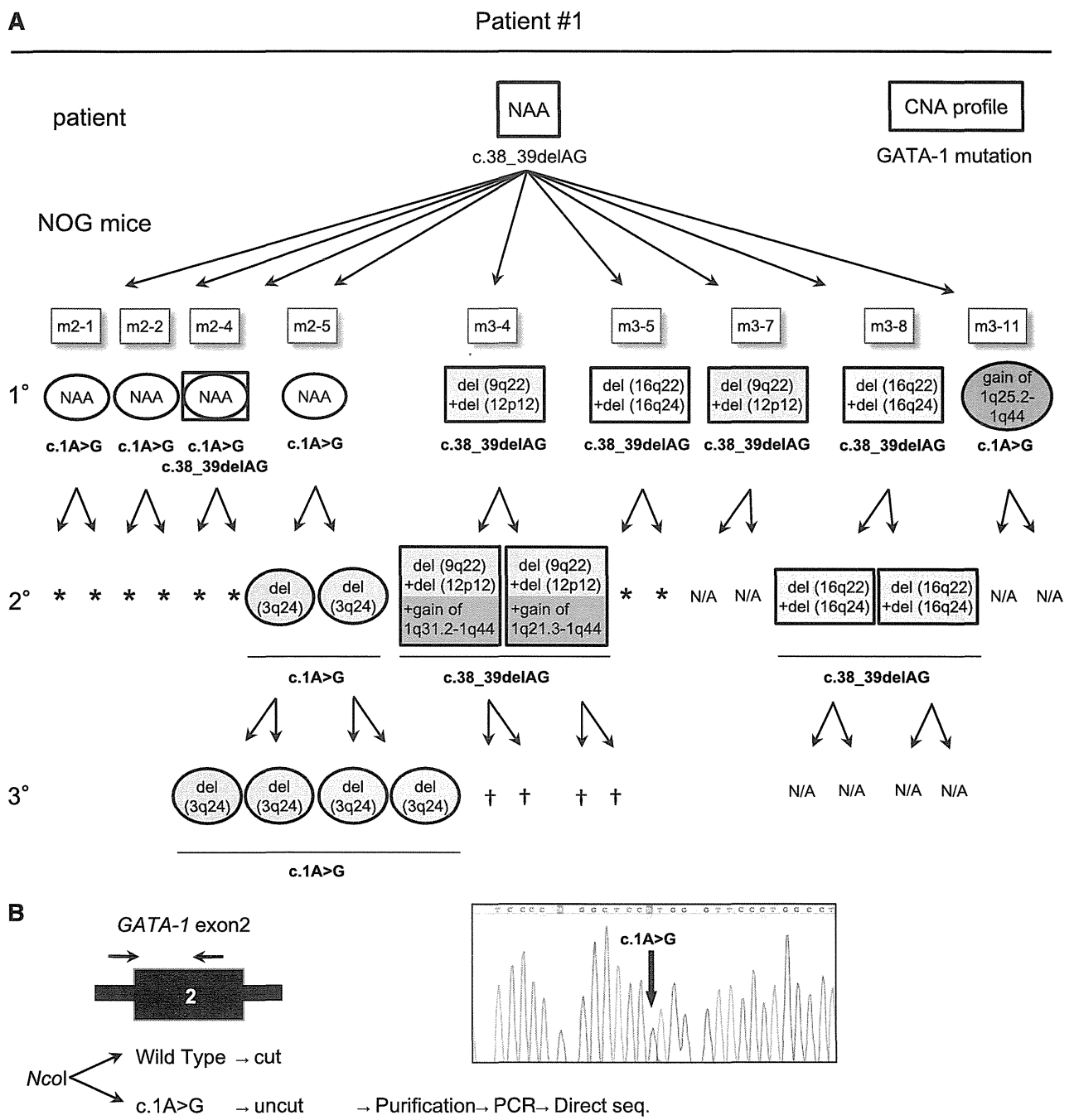

Figure 4. TAM-derived cells show genetic and functional diversity. (A) Summary of the serial transplantation of TAM cells of patient 1 and the results of CNA profiling and *GATA1* mutation analysis. The original patient sample had a single *GATA1* mutation, c.38G_39delAG, and no additional CNAs. Diverse subpopulations with or without additional CNAs expanded in each recipient. *GATA1* mutation analysis showed 2 distinct mutations in recipients: one identical to that of the original patient (c.38_39delAG) and a different mutation (c.1A>G). The mice harboring cells with the original mutation (c.38_39delAG) are shown in rectangles, and the mice with cells harboring the other mutation (c.1A>G) are shown in ovals, with a CNA profile note inside. The *GATA1* mutation is indicated below the symbol. NAA, no additional alteration; N/A, not assessed because of low blast cell count. †Death of recipient before analysis. *No engraftment. (B) Detection of a minor clone with the c.1A>G mutation in the original sample of patient 1. NcoI digestion of a DNA fragment obtained by PCR of *GATA1* exon 2 yielded 2 fragments in the wild type, whereas the mutant allele (c.1A>G) remained undigested. PCR of the undigested band and direct sequence analysis identified the same *GATA1* mutation (c.1A>G mutation) in the patient sample. Black arrow indicates the primer set.

The same method was used to detect a subclone with a 3q24 deletion in the primary patient sample (m2-5; Figure 4A; supplemental Figure 6). At the site of the deletion, genomic breakage was confirmed, and the ends were bound by insertion of a G-nucleotide (Figure 5C; supplemental Figure 7). Consistent with the results of CNA profiling, PCR using DNA from engrafted cells in the 2° and 3° mice (m2-5; Figure 4A) produced a bright DNA fragment, which was confirmed to contain the deletion breakpoint in 3q24 by Sanger sequencing (Figure 5D). Engrafted cells from the BM of the 1° recipient produced a faint DNA fragment, although CNAs were not detected in these cells by array-based methods. We could not detect the corresponding DNA fragment in the primary sample of patient 1. These results suggest the subclone with the 3q24 deletion arose in the 1° recipient mouse as a minor population, emerged as a major population in the 2° recipient, and subsequently engrafted into the 3° recipients.

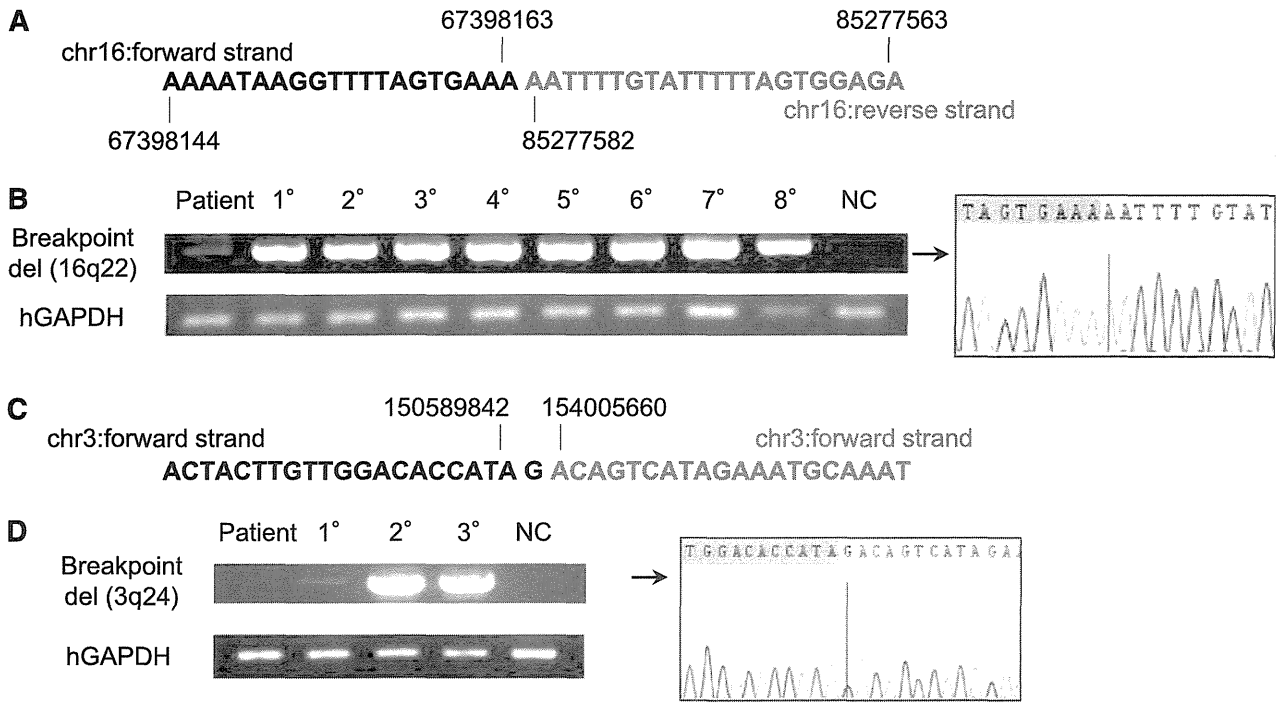

Figure 5. A minor subclone with additional CNAs was present in the primary TAM patient sample, whereas a new clone emerged in a 1° recipient. (A) Contig of del (16q22) breakpoint deduced by whole genome sequencing of the clone containing del(16q22) and del(16q24) in patient 1. Details are shown in supplemental Figure 6. (B) Breakpoint-specific PCR for the del(16q22) clone using genomic DNA from the original patient sample (1; PB in TAM phase), 1° to 8° xenografts (hCD45$^+$ BM cells; Figure 3), and NC (negative control; PBMCs from a healthy adult). Cells from 1° to 8° recipients showed a bright band. The original patient sample showed a faint band, and direct sequencing revealed the presence of the deduced breakpoint for del(16q22). Human glyceraldehyde-3-phosphate dehydrogenase (hGAPDH) was used as an internal control. (C) Contig of del(3q24) breakpoint deduced by whole-genome sequencing. Details are shown in supplemental Figure 9. (D) Breakpoint-specific PCR for the del(3q24) clone using genomic DNA from the original patient sample (1; PB in TAM phase), 1° to 3° xenografts (hCD45$^+$ BM cells, m2–5; Figure 4A), and NC. Cells from 2° and 3° recipients showed a bright band. No band was detected in the original patient sample, but a faint band was detected in the 1° recipient sample. hGAPDH was used as an internal control. Direct sequencing confirmed the presence of cells with the deduced breakpoint for del(3q24) in the 1° recipient.

However, because the sensitivity of the specific PCR targeting of the 3q24 deletion was ~0.1% as determined by the dilution assay (data not shown), it is also possible that this minor clone already existed in the primary patient sample at a frequency below the sensitivity limit. Collectively, our results provide evidence that subclones with additional genetic alterations already exist in the TAM phase and suggest that clonal selection occurs continuously in this xenograft model.

TAM cells derived from patients who did not develop ML-DS had limited self-renewal capacity and fewer additional CNAs than those from the patient who developed ML-DS

To assess whether TAM cells derived from the patients who did not develop ML-DS had similar self-renewal capacity and genetic instability to those from patient 1, CNA analysis of TAM-derived cells was performed by transplanting the preserved PBMC samples of patients 2 and 9. In patient 2, 4 1° transplantation attempts resulted in successful engraftment. The primary sample of patient 2 had no CNAs (Figure 6A). However, TAM-derived cells in 1 of the 1° recipients (m2-2) showed 7p and 7q deletions, suggesting that a subclone with these CNAs may exist in the primary patient sample. The other 2 1° recipients had no additional CNAs (m2-1 and m3-6). In patient 9, engraftment succeeded in 5 1° recipients, and no additional CNAs were detected in either primary patient sample or engrafted TAM-derived cells (Figure 6B). The engrafted cells in all of the recipient mice harbored the same *GATA1* mutation as that of the primary samples of patients 2 and 9. In these 2 cases, our xenograft assay did not detect potent TAM clones with self-renewal capacity in serial transplantation assays (Figure 6A-B; supplemental Table 1), which may reflect the favorable clinical outcome of these patients.

Taken together, the results show that only the TAM cells derived from patients who subsequently developed ML-DS had long-term self-renewal capacity with additional CNAs in our serial transplantation assay.

Discussion

New genomic technologies have led to a better understanding of the complex clonal architecture of leukemia and have shown that disease progression occurs through clonal evolution.[20-22,32] However, most studies have been based on the retrospective analysis of frank leukemia samples, and data on the evolutionary process occurring in the preleukemic phase are limited because primary preleukemia samples are rarely available and are difficult to maintain in vitro or in vivo. TAM is a unique hematologic condition associated with DS that is mostly self-limited but leads to ML-DS in 20% of cases after spontaneous remission. Therefore, TAM has been considered a preleukemic state and is a suitable pathological condition to analyze the evolutionary process of leukemia.

Because mice models in which primary human leukemic cells were transplanted into immunodeficient hosts provided significant clues to advance our understanding of the pathogenesis of human

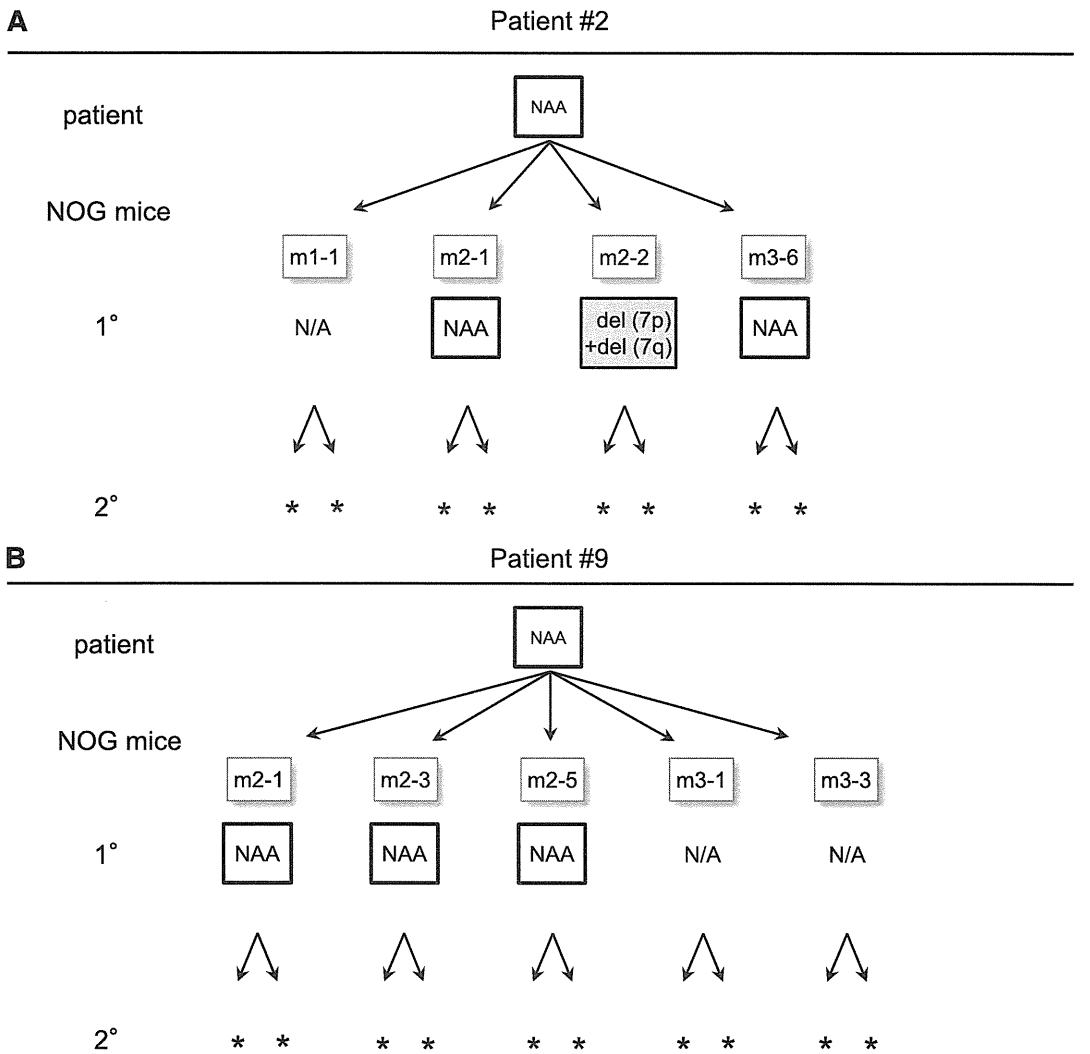

Figure 6. Serial transplantation and CNA profiling of TAM-derived cells from patients that did not develop ML-DS. (A) Serial transplantation assay using TAM cells from patient 2. Four attempts resulted in successful analysis in 1° recipients. CNAs with del(7p) and del(7q) were observed in 1 recipient (m2-2). No additional CNAs were observed in any other recipients. No engraftment was observed in 2° recipients. (B) Serial transplantation assay of TAM cells from patient 9. Five attempts resulted in successful analysis in 1° recipients. No additional CNAs were observed in any analyzed recipients, and no engraftment was observed in 2° recipients. NAA, no additional alteration; N/A, not assessed because of low cell count. *No engraftment.

leukemia,[19-22] we hypothesized that xenograft models of TAM cells would be an attractive method to investigate leukemogenesis. In this report, we demonstrated the long-term engraftment of primary TAM cells in NOG mice and showed that TAM cells from a patient that subsequently developed ML-DS had the potential to gain diverse additional genomic alterations and self-renewal capacity. Although we were unable to determine whether the clonal evolution of TAM cells observed in our model reflected the clinical phenotype of the original patient because of insufficient sample from the ML-DS phase, our model is likely to enable the prospective evaluation of leukemic evolution and can be a powerful tool to study the pathophysiology of leukemogenesis. Our model using NOG mice contrasts somewhat with the study by Chen et al,[27] who reported that TAM cells resided only in the BM after intra-BM infusion into NOD/SCID mice. We speculate that a severe and unique immunodeficient microenvironment may have contributed to the successful engraftment of TAM cells in NOG mice.

In the present study, primary TAM cell samples from 3 of 11 patients engrafted in NOG mice (Figure 1), but serial engraftment was successful only with cells obtained from the patient who developed ML-DS at the age of 1 year (Figures 2, 3, and 6). The results of extensive serial transplantation revealed the emergence of subclones with various additional CNAs characteristic of ML-DS (Figures 3 and 4). Furthermore, we showed that minor subclones with various CNAs and a distinct *GATA1* mutation were already present in the ML-DS patient during the early TAM phase (Figures 4 and 5), as previously described for polyclonality of TAM.[2,33] These findings suggest that several preleukemic clones with high leukemia-initiating potential may already reside as minor clones in TAM cells of patients fated to develop ML-DS and show high repopulating capacity in the special microenvironment of NOG mice. Our findings support the hypothesis that ML-DS develops from a pool of heterogeneous minor clones through clonal selection, illustrating the early evolutionary process of leukemia.[34]

Long-term engraftment of TAM-derived cells was observed for only a minority of TAM patients. This finding suggests that factors other than the properties of the TAM-derived cells, such as technical issues, affected engraftment efficiency. In this regard, increasing the number of transplanted cells resulted in a higher rate of engraftment in recipients of samples from patient 9 (supplemental Table 1).

However, there was no clear association between the percentage of TAM blast cells in transplanted samples and successful engraftment (supplemental Table 1). Likewise, frozen samples from 3 patient samples (patients 1, 2, and 9) were as efficient for engraftment as fresh samples from these patients. Therefore, although the number of injected TAM cells and technical issues may affect engraftment, we speculate that engraftment efficiency is an intrinsic property of each TAM-derived cell population.

In addition to trisomy 21, somatic *GATA1* mutation is considered an early essential event of TAM and ML-DS occurring in utero.[35,36] Interestingly, our TAM-NOG mice model enhanced the emergence of a minor clone with a distinct *GATA1* mutation that was not detectable in the original patient sample by conventional sequencing methods. In our model, a minor *GATA1* mutant clone expanded predominantly in some recipients and acquired CNAs independently of clones with the original *GATA1* mutation, raising the possibility that leukemic evolution occurred from this minor clone, similar to the clinical observation in our previous report.[13] In this scenario, a common founder clone of TAM/ML-DS may be established before the acquisition of the *GATA1* mutation, or TAM clones with distinct *GATA1* mutations may arise independently in the fetal period.

It has long been considered that the linear sequential acquisition of genetic alterations induces disease progression in TAM/ML-DS.[37] By contrast, recent studies using high-throughput genomic technology indicate that evolutionary trajectories are more complex and branching in other cancers and leukemias, as previously proposed by Nowell.[38] In this theory, genomic instability in founder cells gives rise to heterogeneous mutant subclones, and under selective pressure, some subclones expand to result in disease progression, whereas others become extinct or remain dormant. Thus, leukemic clones may evolve and emerge through the complex interaction of selectively advantageous "driver" mutations, additional advantageous "cooperating" mutations, neutral "passenger" mutations, and deleterious mutations.[32,38] It is clinically true that genomic alterations are more frequently observed in ML-DS than in TAM.[2,11,39] In this paper, we showed that diverse subclones with various CNAs can be generated in TAM, and these events occurred preferentially in a patient who later developed ML-DS. These findings suggest the presence of leukemic driver mutations in the early phase of TAM in this patient, which may have induced genomic instability. We were unable to find any candidate tumor-associated genes on the deletion sites (3q24, 9q22, 12p12, 16q22, and 16q24) of TAM-derived cells using the The National Center for Biotechnology Information database, suggesting that other genetic mutations and epigenetic events may contribute to the progression to ML-DS, including a few candidate mutations identified previously.[40-42] It is also noteworthy that subclones in each recipient mouse showed different repopulating capacities in this study. The dominant clones in each recipient were not always identical in the 1° generations, and the dominant clone in a certain recipient did not always propagate dominantly in the next generation recipients (Figure 4A). Differences between the recipient mice or technical problems may have caused variations in engraftment outcome, which is a potential weakness of this xenograft model; however, it is more likely that cooperating genetic event(s) important for leukemogenesis led to the cells of a specific TAM clone becoming the dominant population in each recipient. Such cooperating event(s) could have a considerable impact on a preleukemic TAM clone, and clonal selection might occur in a somewhat random manner. Thus, leukemic evolution may depend on random chance to an extent. Our TAM xenograft model may help demonstrate the branching architecture of clonal evolution in a preleukemic phase, which contrasts with a linear and deterministic pattern of evolution.[34,38] Further genomewide analysis is needed to elucidate the true driver or cooperating mutation(s) and unravel the evolutionary process of leukemia.

In conclusion, we established a xenograft model of TAM using highly immunodeficient NOG mice. Our model enabled the observation of clonal selection and expansion of minor mutant TAM clones and is likely to mimic the early phase of the leukemic evolutionary process, demonstrating the striking genetic heterogeneity and the propagating potential of minor clones in a preleukemic phase. Our xenograft model could be valuable tool for gaining insight into the leukemogenesis of ML-DS and for evaluating the prognosis of TAM patients.

Acknowledgments

The authors thank all the TAM patients and their families for their participation. The authors thank Drs Akira Niwa, Masashi Sanada, Hironao Numabe, Tomoki Kawai, Takahiro Yasumi, and Ryuta Nishikomori for technical advice.

This work was supported by grants from the Japanese Ministry of Education, Culture, Sports, Science, and Technology, and from the Japanese Ministry of Health, Labor and Welfare.

Authorship

Contribution: S.S., I.K., T.M., H.F., and K.U. performed sample collection and processing; S.S., K.T., K.Y., and R.W. performed experiments; A.S.-O. performed microarray analysis (accession number GSE44739); Y.S. and S.M. provided expert statistical analysis; S.S., Y.O., and T.T. analyzed results and made the figures; M.I. and T.N. generated NOG mice; and S.S., K.W., H.H., S.A., E.I., S.O., and T.H. designed the research and wrote the paper.

Conflict-of-interest disclosure: The authors declare no competing financial interests.

Correspondence: Toshio Heike, Department of Pediatrics, Graduate School of Medicine, Kyoto University, 54 Kawahara-cho, Shogoin, Sakyo-ku, Kyoto, 606-8507, Japan; e-mail: heike@kuhp.kyoto-u.ac.jp.

References

1. Pine SR, Guo Q, Yin C, Jayabose S, Druschel CM, Sandoval C. Incidence and clinical implications of GATA1 mutations in newborns with Down syndrome. *Blood.* 2007;110(6):2128-2131.
2. Massey GV, Zipursky A, Chang MN, et al; Children's Oncology Group (COG). A prospective study of the natural history of transient leukemia (TL) in neonates with Down syndrome (DS): Children's Oncology Group (COG) study POG-9481. *Blood.* 2006;107(12):4606-4613.
3. Zipursky A, Poon A, Doyle J. Leukemia in Down syndrome: a review. *Pediatr Hematol Oncol.* 1992;9(2):139-149.
4. Hitzler JK. Acute megakaryoblastic leukemia in Down syndrome. *Pediatr Blood Cancer.* 2007;49(7 Suppl):1066-1069.
5. Hitzler JK, Cheung J, Li Y, Scherer SW, Zipursky A. GATA1 mutations in transient leukemia and acute megakaryoblastic leukemia of Down syndrome. *Blood.* 2003;101(11):4301-4304.
6. Wechsler J, Greene M, McDevitt MA, Anastasi J, Karp JE, Le Beau MM, Crispino JD. Acquired mutations in GATA1 in the megakaryoblastic leukemia of Down syndrome. *Nat Genet.* 2002;32(1):148-152.

7. Groet J, McElwaine S, Spinelli M, et al. Acquired mutations in GATA1 in neonates with Down's syndrome with transient myeloid disorder. *Lancet.* 2003;361(9369):1617-1620.
8. Xu G, Nagano M, Kanezaki R, et al. Frequent mutations in the GATA-1 gene in the transient myeloproliferative disorder of Down syndrome. *Blood.* 2003;102(8):2960-2968.
9. Weiss MJ, Orkin SH. Transcription factor GATA-1 permits survival and maturation of erythroid precursors by preventing apoptosis. *Proc Natl Acad Sci USA.* 1995;92(21):9623-9627.
10. Ferreira R, Ohneda K, Yamamoto M, Philipsen S. GATA1 function, a paradigm for transcription factors in hematopoiesis. *Mol Cell Biol.* 2005; 25(4):1215-1227.
11. Hayashi Y, Eguchi M, Sugita K, et al. Cytogenetic findings and clinical features in acute leukemia and transient myeloproliferative disorder in Down's syndrome. *Blood.* 1988;72(1):15-23.
12. Forestier E, Izraeli S, Beverloo B, et al. Cytogenetic features of acute lymphoblastic and myeloid leukemias in pediatric patients with Down syndrome: an iBFM-SG study. *Blood.* 2008; 111(3):1575-1583.
13. Xu G, Kato K, Toki T, Takahashi Y, Terui K, Ito E. Development of acute megakaryoblastic leukemia from a minor clone in a Down syndrome patient with clinically overt transient myeloproliferative disorder. *J Pediatr Hematol Oncol.* 2006;28(10): 696-698.
14. Vyas P, Crispino JD. Molecular insights into Down syndrome-associated leukemia. *Curr Opin Pediatr.* 2007;19(1):9-14.
15. Kirsammer G, Jilani S, Liu H, Davis E, Gurbuxani S, Le Beau MM, Crispino JD. Highly penetrant myeloproliferative disease in the Ts65Dn mouse model of Down syndrome. *Blood.* 2008;111(2): 767-775.
16. Carmichael CL, Majewski IJ, Alexander WS, Metcalf D, Hilton DJ, Hewitt CA, Scott HS. Hematopoietic defects in the Ts1Cje mouse model of Down syndrome. *Blood.* 2009;113(9): 1929-1937.
17. Alford KA, Slender A, Vanes L, et al. Perturbed hematopoiesis in the Tc1 mouse model of Down syndrome. *Blood.* 2010;115(14):2928-2937.
18. Malinge S, Bliss-Moreau M, Kirsammer G, Diebold L, Chlon T, Gurbuxani S, Crispino JD. Increased dosage of the chromosome 21 ortholog Dyrk1a promotes megakaryoblastic leukemia in a murine model of Down syndrome. *J Clin Invest.* 2012;122(3):948-962.
19. Bonnet D, Dick JE. Human acute myeloid leukemia is organized as a hierarchy that originates from a primitive hematopoietic cell. *Nat Med.* 1997;3(7):730-737.
20. Clappier E, Gerby B, Sigaux F, et al. Clonal selection in xenografted human T cell acute lymphoblastic leukemia recapitulates gain of malignancy at relapse. *J Exp Med.* 2011;208(4): 653-661.
21. Notta F, Mullighan CG, Wang JCY, et al. Evolution of human BCR-ABL1 lymphoblastic leukaemia-initiating cells. *Nature.* 2011; 469(7330):362-367.
22. Anderson K, Lutz C, van Delft FW, et al. Genetic variegation of clonal architecture and propagating cells in leukaemia. *Nature.* 2011;469(7330):356-361.
23. Hiramatsu H, Nishikomori R, Heike T, Ito M, Kobayashi K, Katamura K, Nakahata T. Complete reconstitution of human lymphocytes from cord blood CD34+ cells using the NOD/SCID/gammacnull mice model. *Blood.* 2003;102(3):873-880.
24. Fujino H, Hiramatsu H, Tsuchiya A, et al. Human cord blood CD34+ cells develop into hepatocytes in the livers of NOD/SCID/gamma(c)null mice through cell fusion. *FASEB J.* 2007;21(13):3499-3510.
25. Kato M, Sanada M, Kato I, et al. Frequent inactivation of A20 in B-cell lymphomas. *Nature.* 2009;459(7247):712-716.
26. Kato I, Niwa A, Heike T, et al. Identification of hepatic niche harboring human acute lymphoblastic leukemic cells via the SDF-1/ CXCR4 axis. *PLoS ONE.* 2011;6(11):e27042.
27. Chen J, Li Y, Doedens M, Wang P, Shago M, Dick JE, Hitzler JK. Functional differences between myeloid leukemia-initiating and transient leukemia cells in Down's syndrome. *Leukemia.* 2010;24(5):1012-1017.
28. Ito M, Hiramatsu H, Kobayashi K, et al. NOD/ SCID/gamma(c)(null) mouse: an excellent recipient mouse model for engraftment of human cells. *Blood.* 2002;100(9):3175-3182.
29. Lacombe F, Durrieu F, Briais A, et al. Flow cytometry CD45 gating for immunophenotyping of acute myeloid leukemia. *Leukemia.* 1997;11(11): 1878-1886.
30. Suda J, Eguchi M, Akiyama Y, et al. Differentiation of blast cells from a Down's syndrome patient with transient myeloproliferative disorder. *Blood.* 1987;69(2):508-512.
31. Silva ML, do Socorro Pombo-de-Oliveira M, Raimondi SC, et al. Unbalanced chromosome 1 abnormalities leading to partial trisomy 1q in four infants with Down syndrome and acute megakaryocytic leukemia. *Mol Cytogenet.* 2009;2:7.
32. Welch JS, Ley TJ, Link DC, et al. The origin and evolution of mutations in acute myeloid leukemia. *Cell.* 2012;150(2):264-278.
33. Ahmed M, Sternberg A, Hall G, et al. Natural history of GATA1 mutations in Down syndrome. *Blood.* 2004;103(7):2480-2489.
34. Greaves M, Maley CC. Clonal evolution in cancer. *Nature.* 2012;481(7381):306-313.
35. Shimada A, Xu G, Toki T, Kimura H, Hayashi Y, Ito E. Fetal origin of the GATA1 mutation in identical twins with transient myeloproliferative disorder and acute megakaryoblastic leukemia accompanying Down syndrome. *Blood.* 2004; 103(1):366.
36. Hitzler JK, Zipursky A. Origins of leukaemia in children with Down syndrome. *Nat Rev Cancer.* 2005;5(1):11-20.
37. Khan I, Malinge S, Crispino J. Myeloid leukemia in Down syndrome. *Crit Rev Oncog.* 2011;16(1-2): 25-36.
38. Nowell PC. The clonal evolution of tumor cell populations. *Science.* 1976;194(4260):23-28.
39. Blink M, van den Heuvel-Eibrink MM, Aalbers AM, et al. High frequency of copy number alterations in myeloid leukaemia of Down syndrome. *Br J Haematol.* 2012;158(6):800-803.
40. Malkin D, Brown EJ, Zipursky A. The role of p53 in megakaryocyte differentiation and the megakaryocytic leukemias of Down syndrome. *Cancer Genet Cytogenet.* 2000;116(1):1-5.
41. Norton A, Fisher C, Liu H, et al. Analysis of JAK3, JAK2, and C-MPL mutations in transient myeloproliferative disorder and myeloid leukemia of Down syndrome blasts in children with Down syndrome. *Blood.* 2007;110(3):1077-1079.
42. Malinge S, Ragu C, Della-Valle V, et al. Activating mutations in human acute megakaryoblastic leukemia. *Blood.* 2008;112(10):4220-4226.

OPEN ACCESS Freely available online

PLOS ONE

Robust and Highly-Efficient Differentiation of Functional Monocytic Cells from Human Pluripotent Stem Cells under Serum- and Feeder Cell-Free Conditions

Masakatsu D. Yanagimachi[1,4], Akira Niwa[1], Takayuki Tanaka[1], Fumiko Honda-Ozaki[1], Seiko Nishimoto[1], Yuuki Murata[3], Takahiro Yasumi[3], Jun Ito[1], Shota Tomida[1], Koichi Oshima[1], Isao Asaka[2], Hiroaki Goto[4], Toshio Heike[3], Tatsutoshi Nakahata[1], Megumu K. Saito[1]*

1 Department of Clinilcal Application, Center for iPS Cell Research and Application, Kyoto University, Kyoto, Japan, **2** Department of Fundamental Cell Technology, Center for iPS Cell Research and Application, Kyoto University, Kyoto, Japan, **3** Department of Pediatrics, Kyoto University Graduate School of Medicine, Kyoto, Japan, **4** Department of Pediatrics, Yokohama City University Graduate School of Medicine, Yokohama, Japan

Abstract

Monocytic lineage cells (monocytes, macrophages and dendritic cells) play important roles in immune responses and are involved in various pathological conditions. The development of monocytic cells from human embryonic stem cells (ESCs) and induced pluripotent stem cells (iPSCs) is of particular interest because it provides an unlimited cell source for clinical application and basic research on disease pathology. Although the methods for monocytic cell differentiation from ESCs/iPSCs using embryonic body or feeder co-culture systems have already been established, these methods depend on the use of xenogeneic materials and, therefore, have a relatively poor-reproducibility. Here, we established a robust and highly-efficient method to differentiate functional monocytic cells from ESCs/iPSCs under serum- and feeder cell-free conditions. This method produced $1.3\times10^6\pm0.3\times10^6$ floating monocytes from approximately 30 clusters of ESCs/iPSCs 5–6 times per course of differentiation. Such monocytes could be differentiated into functional macrophages and dendritic cells. This method should be useful for regenerative medicine, disease-specific iPSC studies and drug discovery.

Citation: Yanagimachi MD, Niwa A, Tanaka T, Honda-Ozaki F, Nishimoto S, et al. (2013) Robust and Highly-Efficient Differentiation of Functional Monocytic Cells from Human Pluripotent Stem Cells under Serum- and Feeder Cell-Free Conditions. PLoS ONE 8(4): e59243. doi:10.1371/journal.pone.0059243

Editor: Katriina Aalto-Setala, University of Tampere, Finland

Received August 14, 2012; **Accepted** February 13, 2013; **Published** April 3, 2013

Funding: Funding was provided by grants from the Ministry of Health, Labour and Welfare to TN, a grant from the Ministry of Education, Culture, Sports, Science and Technology (MEXT) to TN, grants from the Leading Project of MEXT to TN, a grant from Funding Program for World-Leading Innovative Research and Development on Science and Technology (FIRST Program) of Japan Society for the Promotion of Science (JSPS) to TN, grants from JSPS to TN and MKS, grants from the Takeda foundation, Mitsubishi Pharma Research Foundation and Suzuken memorial foundation to MKS and grants from Grants-in-Aid for Scientific Research from Japan Society for the Promotion of Science from the Ministry of Education, Culture, Sports, Science, and Technology of Japan to MDY. The funders had no role in study design, data collection and analysis, decision to publish, or preparation of the manuscript.

Competing Interests: The authors have declared that no competing interests exist.

* E-mail: msaito@cira.kyoto-u.ac.jp

Introduction

Monocytic lineage cells, such as monocytes, macrophages and dendritic cells (DCs), are central to immune responses and play key roles in various pathological conditions. [1–2] Monocytes are the myeloid progeny of hematopoietic stem/progenitor cells [3]; they are a type of mononuclear cell circulating in the bloodstream and act as gatekeepers in innate immunity. While they replenish macrophages and DCs, monocytes themselves respond to various inflammatory stimuli by migrating into inflamed tissues, phagocytosing pathological small particles and producing proinflammatory cytokines and chemokines. Therefore, monocytes not only contribute to host defense against pathogenic microorganisms, but are closely associated with the pathogenesis of chronic sterile inflammation. [4] Macrophages reside in tissues and robustly phagocytose microorganisms and cellular debris. One of the important hallmarks of monocytic lineage cells is their functional plasticity. In response to cytokines and microbial products, macrophages polarize into functionally distinct M1 and M2 cells. [5] Classically activated M1 macrophages are induced by interferon-γ (IFNγ), while alternatively activated M2 macrophages can be induced by IL-4 and IL-13. [2,5] M1 macrophages are generally characterized by high production of proinflammatory cytokines, while M2 are characterized by high production of anti-inflammatory cytokines. DCs are the most powerful antigen-presenting cells and have an indispensable role for the activation of T lymphocytes. Because of their ability to mediate communication between innate and acquired immunity, ex vivo expansion of DCs is expected to be a useful source of material for cancer immunotherapies, such as DC-based vaccines. [6–7] Moreover, recent reports of monocyte and/or DC deficiencies highlight the importance of understanding their development in humans. [8] However, there have been technical limitations for tracing the development of human monocytic cells, or for propagating them ex vivo.

Human embryonic stem cells (ESCs) and induced pluripotent stem cells (iPSCs) are undifferentiated pluripotent cells that can be propagated indefinitely. [9–11] The development of monocytic cells from these pluripotent cells is of particular interest because it would provide an unlimited source of these cells for clinical applications and the examination of disease pathologies. Although the methods for hematopoietic differentiation from ESCs/iPSCs

using embryonic body or feeder co-culture systems have already been established, [12] these methods usually depend on xenogeneic feeder cells and/or animal- or human-derived serum, and therefore have a relatively poor-reproducibility. For instance, batch-to-batch variability of serum or feeder cells can influence the characteristics of *in vitro* differentiated DCs. [13] Here, we describe a novel serum- and feeder cell-free method that robustly and repetitively produces monocytic lineage cells from human ESCs/iPSCs.

Materials and Methods

Cell Culture

This study used human ESCs (cell line: KhES1) and iPSCs (cell lines: 201B7, 253G4, CIRA188Ai-W2, and CB-A11). [10,14–15] 201B7, 253G4 [10] and CIRA188Ai-W2 [15] were previously described. A human ES cell line KhES1 was kindly provided by Dr. Norio Nakatsuji. Human iPS cell lines 201B7 and 253G4 were kindly provided by Dr. Shinya Yamanaka. CB-A11 was established from cord-blood mononuclear cells by using episomal vectors. [16] These ESCs/iPSCs were maintained on tissue culture dishes coated with growth factor-reduced Matrigel (Becton-Dickinson) in mTeSR1 serum-free medium (STEMCELL Technologies).

Monocytic Lineage Cell Differentiation Method

The monocytic lineage differentiation protocol was modified from a previously established hematopoietic differentiation protocol (Figure 1). [17] The protocol consists of 5 sequential steps by which mature MPs and DCs are differentiated from human pluripotent cells in a stepwise manner. In the first step, primitive streak cells were induced from undifferentiated ESCs/iPSCs, which were then differentiated into hemangioblast-like hematopoietic progenitors in the second step. In step 3, expanded hematopoietic progenitors were committed towards initial myeloid differentiation, and then differentiated into the monocytic lineage in step 4. Finally, $CD14^+$ monocytes were differentiated into either MPs or DCs in step 5. The cytokines used in this study were purchased from R&D systems.

Step 1: induction of primitive streak-like cells from undifferentiated human ES/iPS cells with BMP4. BMP4 is an important molecule for the initial stage of mesodermal commitment of pluripotent stem cells in vitro. [17] Undifferentiated ESCs/iPSCs colonies were disseminated onto a 100 mm culture dish coated with growth factor-reduced Matrigel in mTeSR1 medium at a density of about 30 colonies per dish. Individual colonies were grown to a diameter of approximately 1 mm (Day 0), and BMP4 (80 ng/mL) was added to the mTeSR1 medium.

Step 2: generation of KDR^+CD34^+ hemangioblast-like cells with VEGF, basic FGF and SCF. VEGF and SCF have been reported to be important cytokines for development of hemoangiogenic progenitors. [18–19] In this step, we also added basic FGF which enhances the development of mesodermal hematopoietic progenitors. [18,20] The mTeSR1 medium was replaced by StemPro-34 serum-free medium (Gibco) containing 2 mM glutamax (Invitrogen) on day 4, and then was supplemented with the step-2 cytokine cocktail composed of VEGF (80 ng/mL), basic FGF (25 ng/ml), and SCF (100 ng/mL).

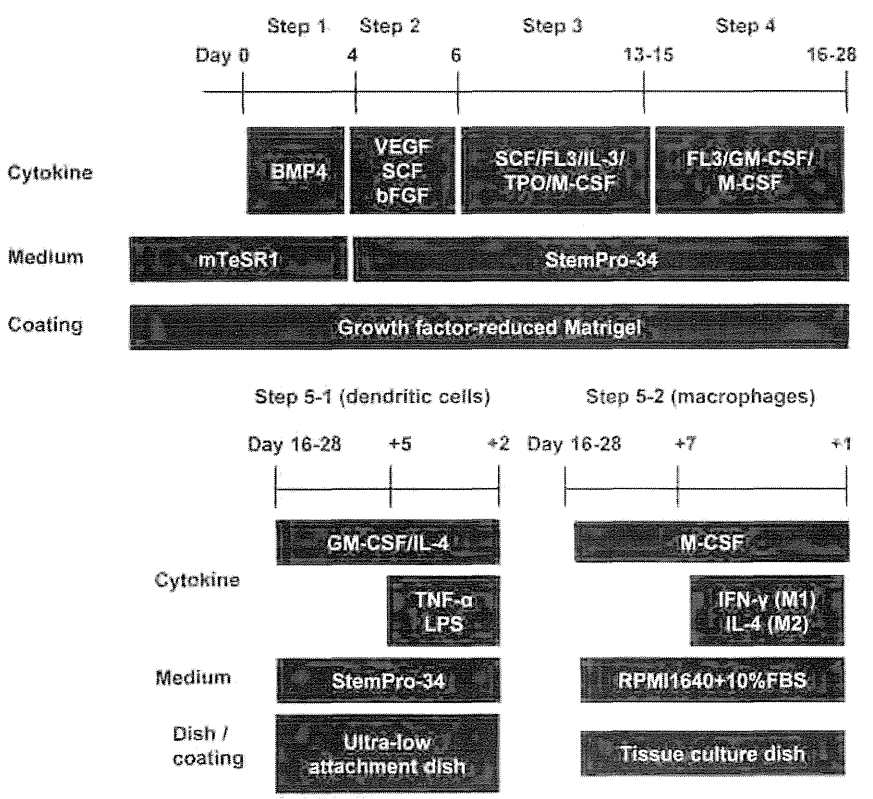

Figure 1. Protocol for monocytic lineage cell differentiation from human pluripotent stem cells. The protocol is composed of 5 steps. CD14-positive cells that are sorted between step-4 are differentiated into dendritic cells by step 5-1 or into macrophages by step 5-2. FL-3: Flt-3 ligand, TPO: Thrombopoietin.
doi:10.1371/journal.pone.0059243.g001

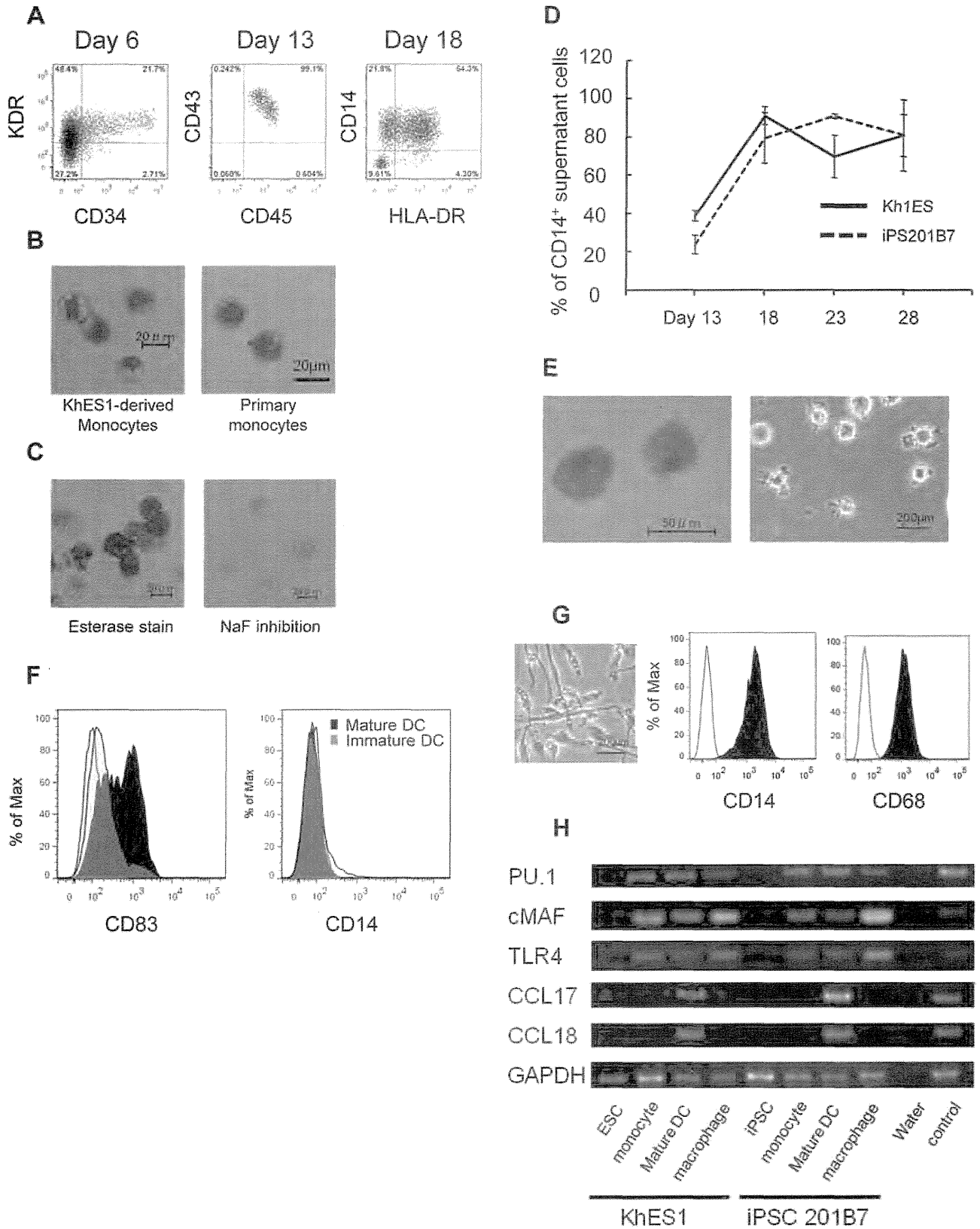

Figure 2. Phenotype analysis and gene expression pattern of monocytic lineage cells derived from pluripotent stem cells. (A) Flow cytometric analysis of monocytic lineage cells derived sequentially from pluripotent stem cells. An analysis of adherent cells on day 6 and supernatant cells on day 13 and 18 is shown. (B) May-Giemsa staining of $CD14^+$ monocyte-like cells derived from KhES1 on day 16 (left) and primary human monocytes (right). (C) Esterase staining for $CD14^+$ monocyte-like cells derived from KhES1 on day 16. (D) The percentage of $CD14^+$ cells within the total floating cells derived from KhES1/iPS-201B7 was evaluated from day 13 to day 28. (E) May-Giemsa staining (left) and phase contrast image (right)

of mature DCs derived from pluripotent stem cells. (F) Flow cytometric analysis of immature/mature DCs derived from pluripotent stem cells. (G) Phase contrast image and flow cytometric analysis of macrophages derived from pluripotent stem cells.(H) RT-PCR analysis of monocytic lineage cells derived from KhES1/iPS-201B7 clones for expression of monocytic lineage marker genes (*PU.1, c-MAF, TLR4, CCL17* and *CCL18*). Peripheral blood monocytes and peripheral blood monocyte-derived mature DCs were used as positive controls.(A–C, E–G) The data from KhES1-derived cells are shown as representative.
doi:10.1371/journal.pone.0059243.g002

Step 3: generation of hematopoietic cells with hematopoietic cytokines. The cytokines in StemPro-34 medium were switched to the step-3 cytokine cocktail composed of SCF (50 ng/mL), IL-3 (50 ng/mL), TPO (Thrombopoietin) (5 ng/mL), M-CSF (50 ng/mL), and Flt-3 ligand (50 ng/mL), on day 6. Thereafter, the medium was changed on day 10.

Step 4: monocytic lineage-directed differentiation with Flt-3 ligand, GM-CSF and M-CSF. The cytokines in StemPro-34 medium were switched to the step-4 cytokine cocktail composed of Flt-3 ligand (50 ng/mL), GM-CSF (25 ng/mL), and M-CSF (50 ng/mL) on day 13–15. The medium was changed every 3–4 days. The $CD14^+$ monocytic lineage-directed cell fraction in supernatant was positively sorted by autoMACS pro (Miltenyi Biotec) with CD14 MicroBeads (Miltenyi Biotec) on days 15–28.

Step 5: differentiation into DCs (step 5-1) and MPs (step 5-2) from $CD14^+$ monocytic lineage-cells. $CD14^+$ cells sorted by autoMACS pro (1.5×10^6 cells per well in a 6-well plate with Ultra-Low Attachment Surface (CORNING)) were cultured in StemPro-34 medium supplemented with GM-CSF (25 ng/mL) and IL-4 (40 ng/mL), with a medium change 4 days later, for differentiation into DCs (step 5-1). LPS (100 ng/mL, InvivoGen) and TNFα (0.2 ng/mL) were added for the last 2 days of the 7 day DC differentiation culture to promote maturation of DCs. $CD14^+$ cells (1.5×10^6 cells per well in a 6-well tissue culture plate) were cultured in RPMI-1640 medium (Sigma) supplemented with 10%

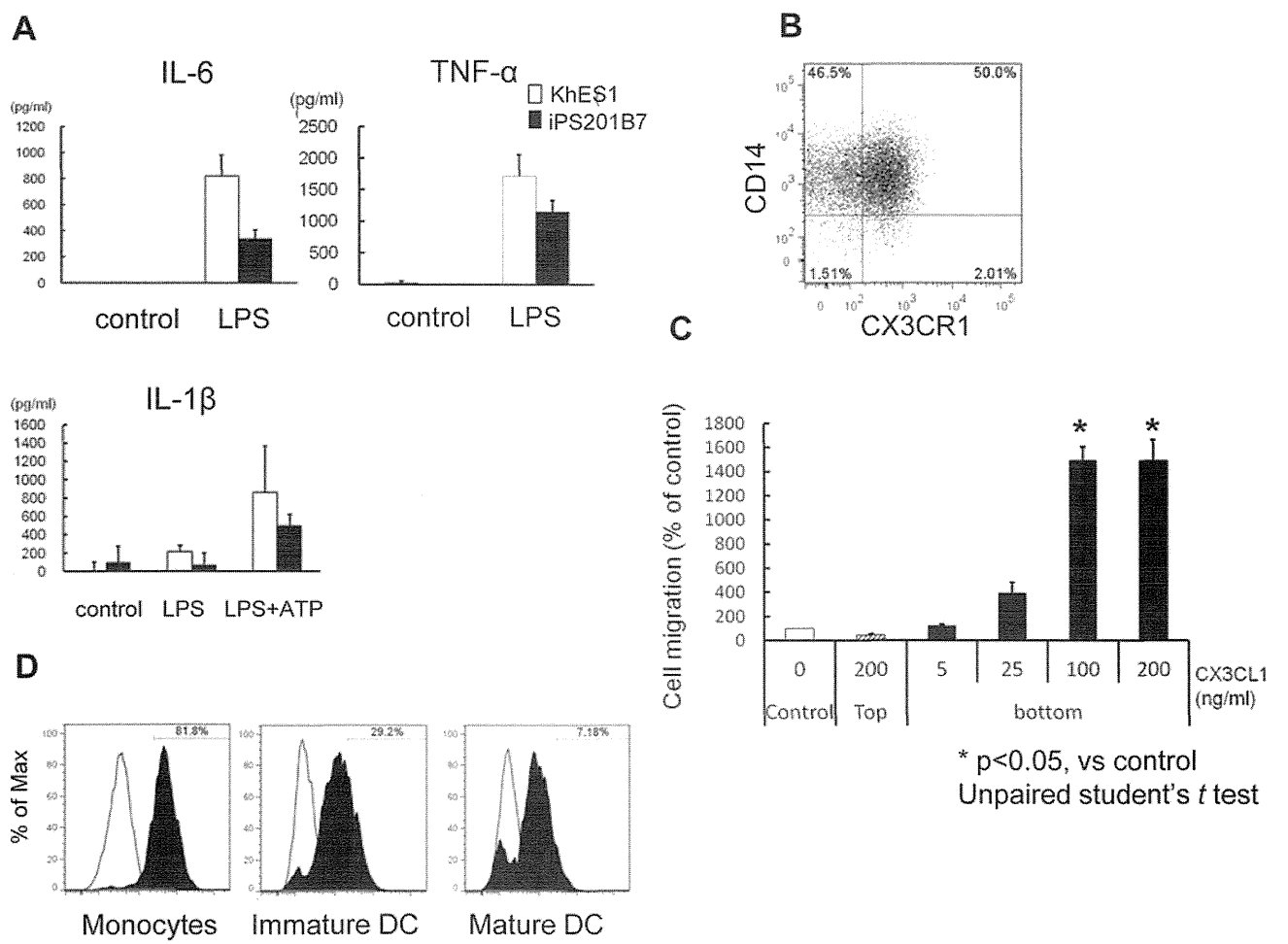

Figure 3. Functional assays for monocytes derived from pluripotent stem cells. (A) The levels of IL-6 and TNFα in supernatants of PS-Mo culture medium 4 hours after LPS stimulation. The levels of IL-1β were measured 4 hours after LPS stimulation with/without an additional 30-minute ATP stimulation. (B) Flow cytometric analysis of CX3CR1 on PS-Mo. (C) Chemotaxis assay of PS-Mo for CX3CL1 (fractalkine) using a trans-well migration assay. After the addition of CX3CL1 into either the bottom or top of the trans-well chamber, PS-Mo were applied and incubated for 5 hours at 37°C. (D) Antigen uptake was evaluated in monocytes, immature DCs and mature DCs derived from pluripotent stem cells by examining the fluorescence intensity of Alexa fluor 488-conjugated ovalbumin 45 minute after incubation at 37°C (black). Control samples (white) were kept on ice. (B–D) The data of KhES1-derived cells are shown as representative. PS-Mo: monocyte derived from pluripotent stem cells.
doi:10.1371/journal.pone.0059243.g003

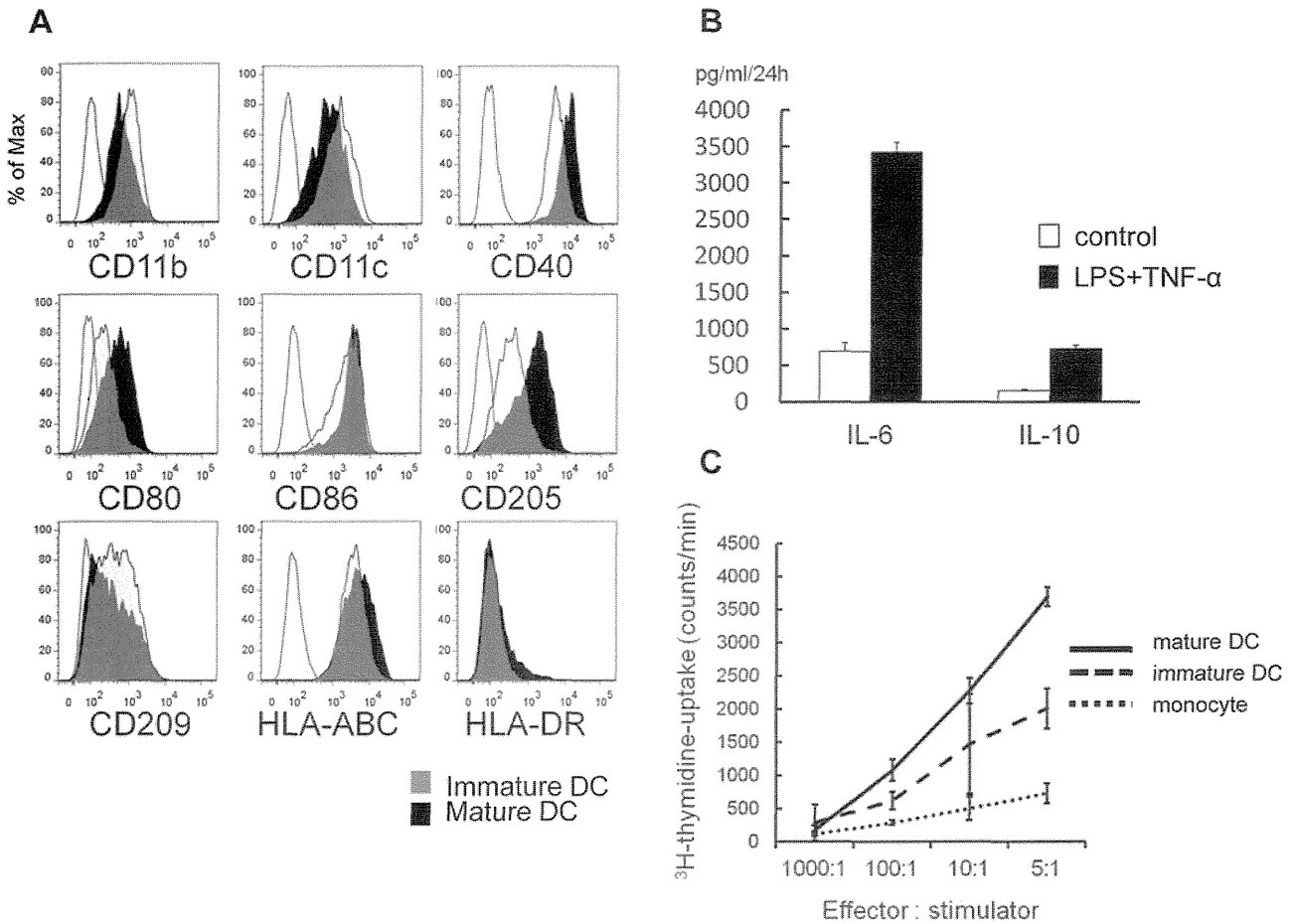

Figure 4. Functional assays for dendritic cells derived from pluripotent stem cells. (A) Flow cytometric analysis of immature/mature DCs derived from pluripotent stem cells. (B) The levels of IL-10 and TNFα in supernatants of culture medium with PS-DCs 24 hours after LPS stimulation. (C) The proliferation of allogeneic naïve T cells (1×10^5 cells per well) co-cultured with 40 Gy-irradiated stimulator cells for 3 days was evaluated. The proliferation of naïve T cells in the last 16 hours was measured by ^{3}H-thymidine uptake. (A–C) The data of KhES1-derived cells are shown as representative.
doi:10.1371/journal.pone.0059243.g004

fetal bovine serum (FBS) and M-CSF (100 ng/mL) for 7 days with a medium change at day 4, for differentiation into macrophages (step 5-2). IFNγ (20 ng/ml) or IL-4 (20 ng/ml) was added for another day to promote differentiation into M1 or M2 macrophages, respectively.

Flow Cytometric Analysis

Flow cytometric analysis data were collected using the MACS Quant™ Analyzer (Miltenyi Biotec) and then analyzed utilizing the FlowJo software package (Treestar). The following antibodies were purchased from BD Biosciences: CD11b-FITC, CD11c-APC, CD34-PE, CD40-PE, CD43-FITC, CD80-PE, CD83-PE, CD86-FITC, CD205-Alexa fluor 647, CD206-FITC, CD209-PE, HLA-ABC-FITC and HLA-DR-FITC. CD14-APC and CD45-APC antibodies were purchased from Beckman Coulter. CD163-APC antibody was purchased from R&D systems. KDR (CD309)-Alexa fluor 647 and CX3CR1-PE antibodies were purchased from Biolegend.

May-Giemsa Staining and Esterase Staining

Cells were seeded onto glass slides by CYTOSPIN 4 (Thermo Scientific) and stained with May-Grunwald and Giemsa staining solution (MERCK) and Esterase staining solution (Muto pure chemicals) following the manufacturer's instructions.

RNA Extraction and RT-PCR Analysis

RNA samples were prepared using the RNeasy mini kit (Qiagen) following the manufacturer's instructions. Typically, 500 ng of total RNA were subjected to reverse transcription (RT) with a Sensiscript-RT kit (Qiagen). RT-PCR was performed for the evaluation of the expression of monocytic lineage marker genes such as *PU.1*, *MAF*, *TLR4*, *CCL17* and *CCL18* using the primers in **Table S1**. [21–22] Peripheral blood monocyte-derived mature DCs/macrophages were generated from peripheral $CD14^+$ monocytes using the step 5-1/5-2 cytokine cocktails in 10% FBS-supplemented RPMI-1640 for use as positive controls.

Cytokine Assay

Concentrations of cytokines (IL-1β, IL-6, IL-10, IL-12p70 and TNFα) in supernatants were analyzed with FlowCytomix kits (Bender MedSystems) following the manufacturer's instructions. The IL-1β, IL-6 and TNFα levels in the culture supernatants of pluripotent cell-derived monocytes (PS-Mo) were analyzed in three settings, (1) culture in RPMI-1640 medium supplemented with 10% FBS and LPS (100 ng/ml) for 4.5 hours, (2) as in (1) but with

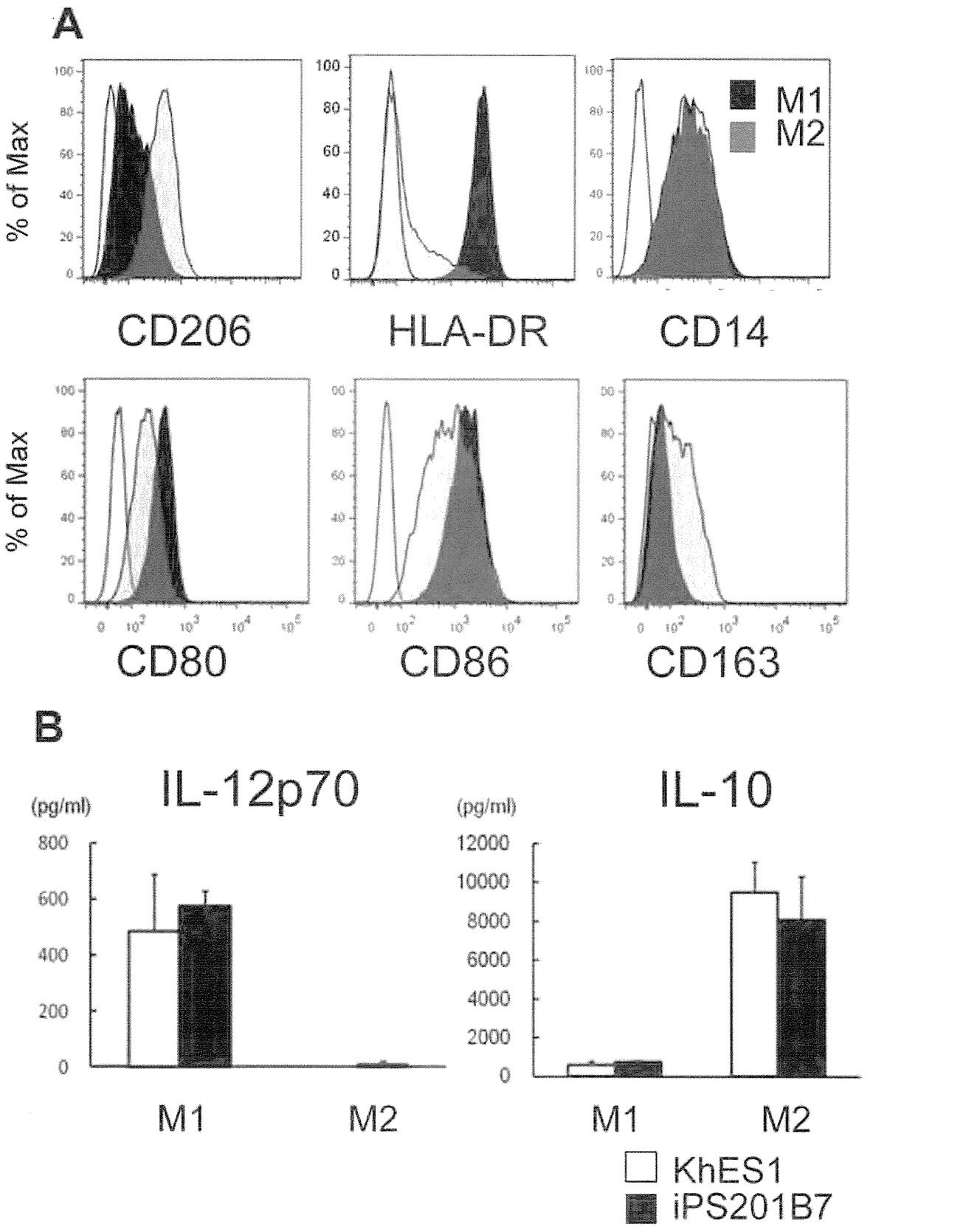

Figure 5. Functional assays for M1/M2 macrophages derived from pluripotent stem cells. (A) Flow cytometric analysis of M1/M2 macrophages derived from pluripotent stem cells. (B) The levels of IL-12p70 and IL-10 in supernatants of culture medium with M1/M2 macrophages derived from pluripotent stem cells 24 hours after LPS stimulation. The data of KhES1-derived cells are shown as representative.
doi:10.1371/journal.pone.0059243.g005

the addition of ATP (1 mM) for the last 30 min, (3) without LPS or ATP for 4.5 hours, to evaluate the production pattern of IL-1β in response to LPS plus ATP. [23].

The levels of IL-6, IL-10, IL-12p70 and TNFα in the supernatants of M1 or M2 macrophage culture were measured 24 hours after LPS (100 ng/ml) stimulation.

Chemotaxis Assay

PS-Mo chemotaxis was evaluated using a trans-well migration assay with 8-μm pore size inserts (BD Biosciences). After CX3CL1 (fractalkine; R&D systems) was added to either the bottom or top of the chamber, serum-starved PS-Mo were loaded onto the inserts which were placed into 24-well plates containing RPMI-1640 and then incubated at 37°C for 5 hours. [24] Cell migration was measured by flow cytometry as previously reported: equivalent amounts of counting beads were added to each sample and the ratios of PS-Mo to the counting beads were calculated. [25].

Antigen Uptake Assay

The antigen uptake capacity of monocytic lineage cells was evaluated as previously described. [26] Briefly, the cells were collected and stored on ice for 10 min. PS-Mo, pluripotent cell-derived immature DCs (PS-imDCs) and pluripotent cell-derived mature DCs (PS-mDCs) (5×10^4 cells) were incubated with Ovalbumin Alexa fluor 488 Conjugate (Molecular Probes) at 0.1 mg/ml at 37°C or on ice for 45 min. Ice-cold FACS buffer was added in order to stop the reaction, samples washed twice, and the fluorescence intensity analyzed by flow cytometry.

Mixed Leukocyte Reactions

Allogeneic naïve T cells (1×10^5 cells per well) were purified from umbilical cord blood mononuclear cells using naïve $CD4^+$ T cell isolation kits (Miltenyi Biotec) and then co-cultured with 40 Gy-irradiated stimulator cells (PS-Mo, PS-imDC, and PS-mDC) in 96-well round bottomed culture plates for 3–5 days. ^{3}H-methylthymidine (25 uCi/ml, Moravek Biochemicals and Radiochemicals) was added to the culture medium of 10% FBS-supplemented RPMI-1640 for the last 16 hours. The cells were harvested onto a filter mat (Perkin Elmer) and the ^{3}H methylthymidine uptake determined using a scintillation counter (MicroBeta TriLux, Perkin Elmer).

Ethical Considerations

This study was approved by the Ethics Committee of Kyoto University and written informed consent was obtained from each healthy volunteer.

Statistics

Data are presented as the mean ± S.D. and the statistical significance of the differences between cultures were evaluated by Student's *t*-test.

Results

Differentiation of ESCs/iPSCs into Dendritic Cells and Macrophages via Monocyte-like Cells

A KDR^+CD34^+ hemangioblast-like population was detected in adherent cell clusters on day 6 (steps 1,2), and around 95% of supernatant cells were $CD43^+CD45^+$ hematopoietic cells on days 13–15 (step 3; **Figure 2A**). [17] Floating cells were recovered every 3–4 days in step 4 (**Figure S1**); the majority of these cells were $CD14^+$ monocyte-like cells (**Figure 2A**). These pluripotent cell-derived monocytes (PS-Mo) were similar to peripheral blood monocytes in morphology (**Figure 2B**). PS-Mo are positive for Esterase staining which was inhibited by NaF (**Figure 2C**). The percentages of PS-Mo in floating cells were constantly about 50–90% between day 18–28 (**Figure 2D and Figure S2A**). The yield of PS-Mo per 100 mm culture dish starting with about 30 colonies was $1.3\times10^6\pm0.3\times10^6$ at each step-4 medium exchange.

To derive DCs, PS-Mo were purified by magnetic sorting, and differentiated into $CD14^-CD83^-$ immature DCs (PS-imDCs) with the step 5-1 cytokine cocktail in 5 days (**Figure 2E**). PS-imDCs were stimulated with LPS and TNFα for an additional 2 days, which further differentiated them into $CD14^-CD83^+$ mature DCs (PS-mDCs) (**Figure 2F**). The differentiation efficiency of mature DCs from PS-Mo was comparable to that from primary monocytes (7.7%±0.9% vs. 16.5%±1.0%, $p=0.20$, unpaired Student's *t*-test). PS-Mo also had the potential to differentiate into macrophages (PS-MPs) with the step 5-2 cytokine cocktail. PS-MPs are morphologically comparable to primary monocyte-derived macrophages and they express typical surface markers such as CD14 and CD68 (**Figure 2G and Figure S3A,B**).

We confirmed that PS-Mo, pluripotent cell-derived DCs (PS-DCs), and PS-MPs expressed monocytic lineage-specific genes (**Figure 2H and Figure S2B**). [22,27] Collectively, by using this protocol, sufficient numbers of monocytic cell lineage cells can be obtained from a small number of human ESCs/iPSCs.

Functional Assays for Monocytes Derived from ESCs/iPSCs

Next, we evaluated the functional activity of pluripotent cell-derived monocytic lineage cells. PS-Mo robustly produced the pro-inflammatory cytokines IL-6 and TNFα after LPS stimulation (**Figure 3A, Figure S3C**). Secretion pattern of IL-1β from PS-Mo with two stepwise signals LPS and ATP were similar to primary monocytes (**Figure 3A, Figure S3D**). [23,28].

PS-Mo expressed CX3CR1, implying chemotactic responses to CX3CL1 (fractalkine) (**Figure 3B**). PS-Mo migration in trans-well assays increased with increasing doses of CX3CL1 in the lower compartment of the chamber (**Figure 3C**). This phenomenon was not due to chemokinesis, but chemotaxis, because CX3CL1 in the top compartment could not induce PS-Mo migration into the lower compartment of the chamber. [24] We next compared the antigen uptake ability of PS-Mo, PS-imDCs, and PS-mDCs by incubating them with Ovalbumin Alexa fluor 488 Conjugate. [26] PS-Mo had the highest ability to take up antigen and as DCs matured they lost their ability to endocytose antigens (**Figure 3D**).

Functional Assays for DCs Derived from ESCs/iPSCs

For evaluating functions of PS-DCs, we first confirmed that patterns of expression of cell surface markers on PS-imDCs/mDCs were comparable to those on primary dendritic cells (**Figure 4A, Figure S4A**). When stimulated with LPS and TNFα, PS-DCs also produced almost comparable amounts of pro-inflammatory and anti-inflammatory cytokines (**Figure 4B, Figure S4B**).

To test the ability of PS-DCs to activate naïve T cells, we next co-cultured allogeneic naïve T cells with PS-DCs and PS-Mo. As shown in Figure 4C, PS-mDCs had the most potent capacity to stimulate allogeneic T cell proliferation and this dose-response relationship was comparable to that observed with PB-DCs (Figure S4C).

Functional Assays for Macrophages Derived from ESCs/iPSCs

Using this technique, we obtained morphologically typical macrophage-like cells that adhered firmly to the culture dish. To test whether these PS-MPs possessed functional plasticity like primary macrophages, we tried to polarize them into M1 or M2 state by treating them with IFNγ or IL-4, respectively. PS-MPs exhibited typical surface markers that were characteristic of primary M1 or M2 macrophages (**Figure 5A, Figure S5A**). The M1 cytokine pattern is typically IL-12^{high} and IL-10^{low}, whereas the M2 pattern is IL-12^{low} and IL-10^{high}. [5] Pluripotent cell-derived M1 and M2 macrophages (PS-M1/M2) also exhibited cytokine profiles that were comparable to those generated from primary monocytes (**Figure 5B, Figure S5B**).

Discussion

We have established a novel differentiation system for monocytic cells from human ES and iPS cells. Since macrophages and dendritic cells are usually obtained *in vitro* from monocytes, the most important point of the evaluation is to establish whether monocytes differentiated from ESCs/iPSCs are functionally comparable to primary monocytes. In several functional assays, PS-Mo indeed proved to be comparable to primary monocytes, and importantly, PS-DCs and PC-MPs from PS-Mo were also functionally comparable to their primary counterparts.

Although complete M1/M2 macrophage polarization still requires aserum-containing medium, the present results prove that the current method can precisely manipulate macrophages that have the potential to differentiate into M1/M2 macrophages. The cytokine profiles of PS-M1/M2 were also comparable to those of primary M1/M2 macrophages. The expression patterns of surface markers in PS-DCs after LPS stimulation and of PS-MPs after M1/M2 polarization were almost identical to those of DCs/MP derived from primary monocytes. However, the level of IL-10 in PS-DCs after stimulation was higher than that in primary DCs and the expression levels of HLA-DR in PS-DCs/MP were low in comparison with those in DCs/MP derived from primary monocytes. Therefore, further improvement of culture conditions such as the use of a modified medium and cytokine cocktail will be needed.

Several embryonic body methods and feeder cell co-culture methods for PS-DCs/MP differentiation have already been reported. [7,27,29–30] These methods show relatively poor-reproducibility because of the use of xenogeneic feeder cells and/or serum. In an earlier report which describes a protocol that can derive macrophages and dendritic cells from human iPSCs in feeder- and serum-free manner, [7] the authors did not fully characterize the monocytes and noted that PS-DCs/MP were generated only from two of the five iPSC clones tested. The current culture system simply propagated progenitor cells in 2-dimensional cultures without passage or sorting, and floating PS-Mo and PS-DCs/MP could be obtained repetitively from all five ESC/iPSC clones tested (**Figure S2 and S6**). These monocytic cells derived from disease- or patient- specific iPSC would be useful tools for the examination of disease pathologies and for drug discovery in immunological disorders such as autoimmune diseases, immunodeficiencies and autoinflammatory syndromes. However, even in our protocol, there are subtle clonal variations of timing of differentiation such as the day of step 3 to 4 switching which is determined by the emergence of CD43^{+}CD45^{+} cells (day 13–15, data not shown). Fine adjustment of the protocol for each ESC/iPSC clone seemed to further improve the yield of monocytes.

iPSC technology is overcoming immunological and ethical concerns in regenerative medicine using human pluripotent cells. Furthermore, a number of disease-associated iPSCs generated from patients with immunological disorders have been reported. [15,31–34] Because patient- or disease-specific iPS cells will be an important resource for unraveling human immunological disorders, a robust and simple hematopoietic differentiation system that can reliably mimic in vivo hematopoiesis is necessary for this purpose. Our simple and robust protocol to produce monocytic cells is therefore expected to be useful for regenerative medicine and studies of immunological disorders.

Supporting Information

Figure S1 Image of floating hematopoietic cells derived from iPS cells Phase contrast image of floating hematopoietic cells derived from iPS-201B7 at day 21 (step 4).
(PDF)

Figure S2 Phenotype analysis and gene expression pattern of monocytic lineage cells derived from 3 additional pluripotent stem cell lines. (A) The percentage of CD14+ cells within the total floating cells derived from 3 iPSC clones (253G4, CIRA188Ai-W2, and CB-A11) was evaluated from day 13 to day 28. (B) RT-PCR analysis of monocytic lineage cells derived from 253G4, CIRA188Ai-W2, and CB-A11 clones for expression of monocytic lineage marker genes (c-MAF, TLR4, and CCL17). Peripheral blood monocytes and peripheral blood monocyte-derived mature DCs were used as positive controls.
(PDF)

Figure S3 Characteristics of primary monocytes and macrophages. (A) Phase contrast image and (B) flow cytometric analysis of macrophages derived from primary monocytes. (C) The levels of IL-6 and TNF-α in supernatants of primary monocyte culture medium 4 hours after LPS stimulation. (D) The levels of IL-1β were measured 4 hours after LPS stimulation with/without an additional 30-minute ATP stimulation.
(PDF)

Figure S4 Characteristics and functional assays of dendritic cells derived from primary monocytes. (A) Flow cytometric analysis of immature/mature DCs derived from primary monocytes. (B) The levels of IL-10 and TNF-α in supernatants of culture medium with primary-DCs 24 hours after LPS stimulation. (C) The proliferation of allogeneic naïve T cells (1×105 cells per well) co-cultured with 40 Gy-irradiated stimulator cells for 3 days was evaluated. The proliferation of naïve T cells in the last 16 hours was measured by 3H-thymidine uptake.
(PDF)

Figure S5 Characteristics and functional assays of M1/M2 macrophages derived from primary monocytes. (A) Flow cytometric analysis of M1/M2 macrophages derived from primary monocytes. (B) The levels of IL-12p70 and IL-10 in supernatants of culture medium with M1/M2 macrophages derived from primary monocytes 24 hours after LPS stimulation.
(PDF)

Figure S6 Replication assays for 3 additional pluripotent stem cell lines. (A) Phase contrast image (left) and May-Giemsa staining (right) of mature DCs derived from iPSC clones. (B) Phase contrast image of macrophages derived from iPSC clones. (C) Flow cytometric analysis of immature/mature DCs and macrophages derived from iPSC clones.
(PDF)

Table S1 Primers for RT-PCR.
(PDF)

Acknowledgments

We are grateful to Y. Sasaki, Y. Jindai, K. Kobayashi, M. Yamane, and S. Nakamura for technical assistance. We would also like to thank N. Takasu and Y. Takao for administrative assistance.

Author Contributions

iPSC establishment: MDY IA. Conceived and designed the experiments: MDY AN HG TH TN MKS. Performed the experiments: MDY ST SN YM TT JI FHO. Analyzed the data: MDY AN TY KO TN MKS. Wrote the paper: MDY AN TY MKS.

References

1. Auffray C, Sieweke MH, Geissmann F (2009) Blood monocytes: development, heterogeneity, and relationship with dendritic cells. Annu Rev Immunol 27: 669–692.
2. Mosser DM, Edwards JP (2008) Exploring the full spectrum of macrophage activation. Nat Rev Immunol 8: 958–969.
3. Geissmann F, Manz MG, Jung S, Sieweke MH, Merad M, et al. (2010) Development of monocytes, macrophages, and dendritic cells. Science 327: 656–661.
4. Ingersoll MA, Platt AM, Potteaux S, Randolph GJ (2011) Monocyte trafficking in acute and chronic inflammation. Trends Immunol 32: 470–477.
5. Mantovani A, Sozzani S, Locati M, Allavena P, Sica A (2002) Macrophage polarization: tumor-associated macrophages as a paradigm for polarized M2 mononuclear phagocytes. Trends Immunol 23: 549–555.
6. Boudreau JE, Bonehill A, Thielemans K, Wan Y (2011) Engineering dendritic cells to enhance cancer immunotherapy. Mol Ther 19: 841–853.
7. Senju S, Haruta M, Matsumura K, Matsunaga Y, Fukushima S, et al. (2011) Generation of dendritic cells and macrophages from human induced pluripotent stem cells aiming at cell therapy. Gene Ther 18: 874–883.
8. Collin M, Bigley V, Haniffa M, Hambleton S (2011) Human dendritic cell deficiency: the missing ID? Nat Rev Immunol 11: 575–583.
9. Thomson JA, Itskovitz-Eldor J, Shapiro SS, Waknitz MA, Swiergiel JJ, et al. (1998) Embryonic stem cell lines derived from human blastocysts. Science 282: 1145–1147.
10. Takahashi K, Tanabe K, Ohnuki M, Narita M, Ichisaka T, et al. (2007) Induction of pluripotent stem cells from adult human fibroblasts by defined factors. Cell 131: 861–872.
11. Yamanaka S (2007) Strategies and new developments in the generation of patient-specific pluripotent stem cells. Cell Stem Cell 1: 39–49.
12. Orlovskaya I, Schraufstatter I, Loring J, Khaldoyanidi S (2008) Hematopoietic differentiation of embryonic stem cells. Methods 45: 159–167.
13. Royer PJ, Tanguy-Royer S, Ebstein F, Sapede C, Simon T, et al. (2006) Culture medium and protein supplementation in the generation and maturation of dendritic cells. Scand J Immunol 63: 401–409.
14. Suemori H, Yasuchika K, Hasegawa K, Fujioka T, Tsuneyoshi N, et al. (2006) Efficient establishment of human embryonic stem cell lines and long-term maintenance with stable karyotype by enzymatic bulk passage. Biochem Biophys Res Commun 345: 926–932.
15. Tanaka T, Takahashi K, Yamane M, Tomida S, Nakamura S, et al. (2012) Induced pluripotent stem cells from CINCA syndrome patients as a model for dissecting somatic mosaicism and drug discovery. Blood.
16. Okita K, Matsumura Y, Sato Y, Okada A, Morizane A, et al. (2011) A more efficient method to generate integration-free human iPS cells. Nat Methods 8: 409–412.
17. Niwa A, Heike T, Umeda K, Oshima K, Kato I, et al. (2011) A novel serum-free monolayer culture for orderly hematopoietic differentiation of human pluripotent cells via mesodermal progenitors. PLoS One 6: e22261.
18. Pick M, Azzola L, Mossman A, Stanley EG, Elefanty AG (2007) Differentiation of human embryonic stem cells in serum-free medium reveals distinct roles for bone morphogenetic protein 4, vascular endothelial growth factor, stem cell factor, and fibroblast growth factor 2 in hematopoiesis. Stem Cells 25: 2206–2214.
19. Umeda K, Heike T, Yoshimoto M, Shiota M, Suemori H, et al. (2004) Development of primitive and definitive hematopoiesis from nonhuman primate embryonic stem cells in vitro. Development 131: 1869–1879.
20. Yu P, Pan G, Yu J, Thomson JA (2011) FGF2 sustains NANOG and switches the outcome of BMP4-induced human embryonic stem cell differentiation. Cell Stem Cell 8: 326–334.
21. Friedman AD (2007) Transcriptional control of granulocyte and monocyte development. Oncogene 26: 6816–6828.
22. Zhong W, Fei M, Zhu Y, Zhang X (2009) Transcriptional profiles during the differentiation and maturation of monocyte-derived dendritic cells, analyzed using focused microarrays. Cell Mol Biol Lett 14: 587–608.
23. Mariathasan S, Weiss DS, Newton K, McBride J, O'Rourke K, et al. (2006) Cryopyrin activates the inflammasome in response to toxins and ATP. Nature 440: 228–232.
24. Gevrey JC, Isaac BM, Cox D (2005) Syk is required for monocyte/macrophage chemotaxis to CX3CL1 (Fractalkine). J Immunol 175: 3737–3745.
25. Morishima T, Watanabe K, Niwa A, Fujino H, Matsubara H, et al. (2011) Neutrophil differentiation from human-induced pluripotent stem cells. J Cell Physiol 226: 1283–1291.
26. Li GB, Lu GX (2010) Adherent cells in granulocyte-macrophage colony-stimulating factor-induced bone marrow-derived dendritic cell culture system are qualified dendritic cells. Cell Immunol 264: 4–6.
27. Choi KD, Vodyanik MA, Slukvin II (2009) Generation of mature human myelomonocytic cells through expansion and differentiation of pluripotent stem cell-derived lin-CD34+CD43+CD45+ progenitors. J Clin Invest 119: 2818–2829.
28. Hogquist KA, Nett MA, Unanue ER, Chaplin DD (1991) Interleukin 1 is processed and released during apoptosis. Proc Natl Acad Sci U S A 88: 8485–8489.
29. Su Z, Frye C, Bae KM, Kelley V, Vieweg J (2008) Differentiation of human embryonic stem cells into immunostimulatory dendritic cells under feeder-free culture conditions. Clin Cancer Res 14: 6207–6217.
30. Tseng SY, Nishimoto KP, Silk KM, Majumdar AS, Dawes GN, et al. (2009) Generation of immunogenic dendritic cells from human embryonic stem cells without serum and feeder cells. Regen Med 4: 513–526.
31. Jiang Y, Cowley SA, Siler U, Melguizo D, Tilgner K, et al. (2012) Derivation and functional analysis of patient-specific induced pluripotent stem cells as an in vitro model of chronic granulomatous disease. Stem Cells 30: 599–611.
32. Park IH, Arora N, Huo H, Maherali N, Ahfeldt T, et al. (2008) Disease-specific induced pluripotent stem cells. Cell 134: 877–886.
33. Pessach IM, Ordovas-Montanes J, Zhang SY, Casanova JL, Giliani S, et al. (2011) Induced pluripotent stem cells: a novel frontier in the study of human primary immunodeficiencies. J Allergy Clin Immunol 127: 1400–1407 e1404.
34. Zou J, Sweeney CL, Chou BK, Choi U, Pan J, et al. (2011) Oxidase-deficient neutrophils from X-linked chronic granulomatous disease iPS cells: functional correction by zinc finger nuclease-mediated safe harbor targeting. Blood 117: 5561–5572.

Int J Hematol (2013) 98:578–588
DOI 10.1007/s12185-013-1429-2

ORIGINAL ARTICLE

Appropriate dose reduction in induction therapy is essential for the treatment of infants with acute myeloid leukemia: a report from the Japanese Pediatric Leukemia/Lymphoma Study Group

Daisuke Tomizawa · Akio Tawa · Tomoyuki Watanabe · Akiko Moriya Saito · Kazuko Kudo · Takashi Taga · Shotaro Iwamoto · Akira Shimada · Kiminori Terui · Hiroshi Moritake · Akitoshi Kinoshita · Hiroyuki Takahashi · Hideki Nakayama · Nobutaka Kiyokawa · Keiichi Isoyama · Shuki Mizutani · Junichi Hara · Keizo Horibe · Tatsutoshi Nakahata · Souichi Adachi

Received: 11 March 2013 / Revised: 4 September 2013 / Accepted: 4 September 2013 / Published online: 26 September 2013

Abstract Infants (<1 year old) with acute myeloid leukemia (AML) are particularly vulnerable to intensive cytotoxic therapy. Indeed, the mortality rate was high among infants enrolled in the Japanese Pediatric Leukemia/Lymphoma Study Group AML-05 study, which prompted us to temporarily suspend patient enrollment and amend the protocol. Forty-five infants with AML were enrolled. For patients aged <2 years, drug doses were adjusted for body weight. Following the protocol amendments, doses for infants were reduced by a further 33 % in the initial induction course. Six infants died during the induction phase (including five early deaths), mainly due to pulmonary complications. The 3-year probability of overall survival (pOS) in all 45 infants [55.9 %, 95 % confidence interval (CI) 37.9–70.6 %] was significantly lower than that of patients aged 1 to <2 years (77.0 %, 95 % CI 62.7–86.3 %) and those aged ≥2 years (74.7 %, 95 % CI 69.2–79.4 %) ($P = 0.037$), mainly due to the higher non-relapse mortality rate in infants. No early deaths occurred after the protocol amendments, and the 3-year pOS of the 17 infants enrolled thereafter was 76.4 % (95 % CI 48.8–90.4 %). In conclusion, appropriate dose reduction is

D. Tomizawa (✉) · S. Mizutani
Department of Pediatrics, Tokyo Medical and Dental University, 1-5-45 Yushima, Bunkyo-ku, Tokyo 113-8519, Japan
e-mail: dtomizawa.ped@tmd.ac.jp

A. Tawa
Department of Pediatrics, National Hospital Organization, Osaka Medical Center, Osaka, Japan

T. Watanabe
Department of Nutritional Science, Faculty of Psychological and Physical Science, Aichi Gakuin University, Aichi, Japan

A. M. Saito · K. Horibe
Clinical Research Center, National Hospital Organization, Nagoya Medical Center, Nagoya, Aichi, Japan

K. Kudo
Division of Hematology and Oncology, Shizuoka Children's Hospital, Shizuoka, Japan

T. Taga
Department of Pediatrics, Shiga University of Medical Science, Otsu, Shiga, Japan

S. Iwamoto
Department of Pediatrics, Mie University School of Medicine, Tsu, Mie, Japan

A. Shimada
Department of Pediatrics, Okayama University, Okayama, Japan

K. Terui
Department of Pediatrics, Hirosaki University Graduate School of Medicine, Hirosaki, Aomori, Japan

H. Moritake
Division of Pediatrics, Department of Reproductive and Developmental Medicine, Faculty of Medicine, University of Miyazaki, Miyazaki, Japan

A. Kinoshita
Department of Pediatrics, St. Marianna University School of Medicine, Kawasaki, Kanagawa, Japan

H. Takahashi
Department of Pediatrics, Toho University, Ota-ku, Tokyo, Japan

H. Nakayama
Department of Pediatrics, National Hospital Organization, Fukuoka-Higashi Medical Center, Koga, Fukuoka, Japan

N. Kiyokawa
Department of Pediatric Hematology and Oncology Research, National Center for Child Health and Development, Setagaya-ku, Tokyo, Japan

essential to avoid early deaths when treating infants with AML.

Keywords Acute myeloid leukemia · Infants · Early death · Acute respiratory distress syndrome

Introduction

Infants aged <1 year with acute myeloid leukemia (AML) show distinct clinical features compared with older children with AML, including a higher white blood cell (WBC) count, extramedullary involvement at diagnosis, and a higher frequency of M4/M5 or M7 leukemic cells classified by the French–American–British (FAB) system, as well as unique cytogenetic characteristics [1, 2]. Relatively few infants have favorable cytogenetic characteristics, such as t(8;21)(q22;q22)/*RUNX1-RUNX1T1*, inv(16)(p13.1q22) or t(16;16)(p13.1;q22)/*CBFB-MYH11*, or t(15;17)(q22;q12)/*PML-RARA*. Most infants have cytogenetic characteristics that are associated with poor prognosis, including rearrangement of the mixed lineage leukemia (*MLL*) gene on chromosome 11q23, t(1;22)(p13;q13)/*RBM15-MKL1*, which is highly associated with acute megakaryocytic leukemia in non-Down syndrome infants, and t(7;12)(q36;p13)/*HLXB9-ETV6* [3–5]. Hence, infants with AML are usually classified in intermediate (IR) or high-risk (HR) groups, and are treated with an intensive combination chemotherapy regimen based on cytarabine and anthracyclines that is also used for older children. However, as infants are particularly vulnerable to intensive cytotoxic treatment, many study groups have modified the doses of chemotherapeutic drugs administered to infants [6, 7].

In the nationwide multicenter AML-05 study conducted by the Japanese Pediatric Leukemia/Lymphoma Study Group (JPLSG), the early mortality rate was unacceptably high among the first 32 infants (28 eligible infants) enrolled in the study, mainly because of acute respiratory distress syndrome (ARDS). This issue prompted us to temporarily suspend patient enrollment and amend the protocol. Here, we report the outcomes of 45 infants with AML who were enrolled and treated in the AML-05 study.

K. Isoyama
Department of Pediatrics, Showa University Fujigaoka Hospital, Yokohama, Kanagawa, Japan

J. Hara
Department of Pediatric Hematology/Oncology, Osaka City General Hospital, Osaka, Japan

T. Nakahata
Center for iPS Cell Research and Application, Kyoto University, Kyoto, Japan

S. Adachi
Human Health Sciences, Kyoto University, Kyoto, Japan

Materials and methods

Patients

Between November 2006 and December 2010, 485 consecutive patients aged <18 years old with suspected AML treated at 118 institutions in Japan were registered in the AML-05 study. Patients with acute promyelocytic leukemia, Down syndrome, secondary AML, myeloid/natural killer cell leukemia, and myeloid sarcoma were not eligible. AML was diagnosed using the World Health Organization (WHO) classification of tumors of hematopoietic and lymphoid tissues (3rd edition) [8] with a comprehensive central diagnostic review system that used morphology, immunophenotyping [9], and cytogenetic analysis of diagnostic bone marrow specimens. Overall, 38 patients (including 5 infants) were excluded, mainly because of misdiagnosis, while 4 additional patients were excluded because the guardian refused to participate ($n = 1$), there was a significant protocol violation during the initial induction course ($n = 1$), the hospital withdrew its membership from the JPLSG ($n = 1$), and the patient was transferred to a non-JPLSG member hospital ($n = 1$). Among the 443 eligible patients, 45 (10.1 %) were infants aged <1 year at initial diagnosis. Written informed consent, provided according to the Declaration of Helsinki, was obtained from the guardians of each patient. All aspects of the study were approved by the institutional review boards at all participating institutions.

Treatments

The therapeutic regimens used in the AML-05 study are presented in Fig. 1. After the second induction course, the patients were stratified to one of three risk groups according to their cytogenetic characteristics and treatment response following the initial induction course, and received three additional intensified chemotherapeutic courses. Patients who failed to achieve complete remission (CR) after the second course were removed from the study. Allogeneic hematopoietic stem cell transplantation (HSCT) was indicated for all of the high-risk (HR) patients after three or more treatment courses. For patients aged <2 years, the drug doses were reduced by taking into account body weight rather than body surface area throughout the treatment course. Because of the high early mortality rate in infants, we temporarily suspended the enrollment of infants between April 2 and August 11, 2009. At this time, the following amendments were made: (1) an

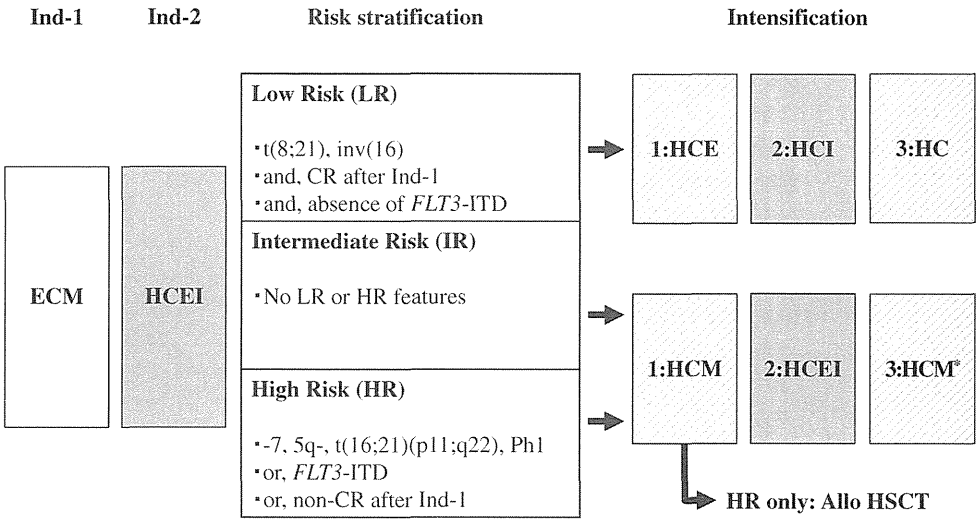

Fig. 1 Treatment schedule in the AML-05 study. ECM consisted of etoposide (150 mg/m^2 per day on days 1–5), cytarabine [200 mg/m^2/day via 12 h continuous intravenous (CIV) infusion on days 6–12], mitoxantrone (5 mg/m^2/day on days 6–10), and an age-adjusted dose of triple intrathecal chemotherapy (TIT) on day 6. HCEI consisted of high-dose cytarabine (HDCA; 3 g/m^2 every 12 h on days 1–3), etoposide (100 mg/m^2/day on days 1–5), idarubicin (10 mg/m^2 on day 1), and TIT on day 1. HCE consisted of HDCA (2 g/m^2 every 12 h on days 1–5), etoposide (100 mg/m^2/day on days 1–5), and TIT on day 1. HCI consisted of HCEI without etoposide. HC consisted of HCE without etoposide. HCM consisted of HDCA (2 g/m^2 every 12 h on days 1–5), mitoxantrone (5 mg/m^2/day on days 1 and 2), and TIT on day 1. *Ind-1* induction course 1, *Ind-2* induction course 2, *Allo HSCT* allogeneic hematopoietic stem cell transplantation. *Asterisk* indicates patients in the intermediate-risk or high-risk groups who experienced Grade 4 infection during intensification course 1 with HCM received HC for intensification course 3

additional dose reduction by 33 % during induction phase 1 for infants; (2) avoidance of the prophylactic administration of granulocyte-colony stimulating factor (G-CSF), considering its possibility as a risk factor for developing ARDS; (3) introduction of enhanced guidelines for supportive care in relation to infection prevention; and (4) close prospective safety monitoring during the induction phase.

Statistical analyses

The baseline characteristics and the clinical course of patients were analyzed using the χ^2 test or Fisher's exact test for categorical variables, and the Wilcoxon rank-sum test for continuous variables. Early death was defined as any-cause death occurring within 42 days of enrollment. Event-free survival (EFS) was defined as the time from the diagnosis of AML to the last follow-up or the first event (failure to achieve remission, relapse, secondary malignancy, or any-cause death). Overall survival (OS) was defined as the time from the diagnosis of AML to any-cause death. The probabilities of EFS (pEFS) and OS (pOS) were estimated using the Kaplan–Meier method. Standard errors (SEs) were calculated using the Greenwood formula and curves were compared using the log-rank test. Confidence intervals (CIs) were calculated at the 95 % confidence level. Gray's methods were used to estimate and compare the cumulative incidence of important events (relapse, non-relapse death). All analyses were performed using STATA® statistical software (version 11.0; StataCorp LP, College Station, TX). Follow-up data were actualized as of May 1, 2012. This trial is registered with the UMIN Clinical Trials Registry (UMIN-CTR, URL: http://www.umin.ac.jp/ctr/index.htm), number UMIN000000511.

Results

Patient characteristics and clinical outcomes according to age group

The characteristics of the patients are reported in Table 1 for three age groups: infants (<1 year old), 1 to <2 years old, and ≥2 years old. Distributions of FAB categories and cytogenetic characteristics differed among the three groups. In particular, there were more patients with monocytic (M5a/M5b) and megakaryocytic (M7) leukemia, but less with M1/M2 leukemia in the younger age groups. Regarding cytogenetic characteristics, there were more patients with *MLL* gene rearrangements [t(9;11) and other 11q23 abnormalities], but fewer with core-binding factor AML [t(8;21) and inv(16)/t(16;16)] among infants compared with the other age groups. None of the infants were positive for *FLT3* internal tandem duplications.

Table 1 Patient characteristics according to age group

	<1 year ($n = 45$) n (%)	1 to <2 years ($n = 58$) n (%)	≥2 years ($n = 340$) n (%)	P value
Sex				
Male	20 (44.4)	32 (55.1)	186 (54.7)	0.419
Female	25 (55.5)	26 (44.8)	154 (45.2)	
WBC at diagnosis (/μL)				
<10,000	8 (17.7)	20 (34.4)	128 (37.6)	0.051
10,000–50,000	25 (55.5)	23 (39.6)	117 (34.4)	
>50,000	12 (26.6)	15 (25.8)	95 (27.9)	
FAB classification				
M0	0 (0.0)	0 (0.0)	8 (2.3)	<0.001
M1	2 (4.4)	3 (5.1)	52 (15.2)	
M2	1 (2.2)	2 (3.4)	114 (33.5)	
M3	1 (2.2)	0 (0.0)	0 (0.0)	
M4	3 (6.6)	4 (6.8)	40 (11.7)	
M4Eo	1 (2.2)	5 (8.6)	9 (2.6)	
M5a	15 (33.3)	11 (18.9)	49 (14.4)	
M5b	4 (8.8)	4 (6.8)	11 (3.2)	
M6	0 (0.0)	5 (8.6)	5 (1.4)	
M7	14 (31.1)	21 (36.2)	13 (3.8)	
RAEB[a]	1 (2.2)	1 (1.7)	1 (0.2)	
RAEB-T[a]	1 (2.2)	2 (3.4)	36 (10.5)	
ND	2 (4.4)	0 (0.0)	2 (0.5)	
Cytogenetic characteristics				
t(8;21)	0 (0.0)	1 (1.7)	121 (35.5)	<0.001
inv(16)	1 (2.2)	6 (10.3)	25 (7.3)	
t(9;11)	8 (17.7)	9 (15.5)	22 (6.4)	
Other 11q23 abnormalities	11 (24.4)	4 (6.8)	15 (4.4)	
t(6;9)	0 (0.0)	0 (0.0)	3 (0.8)	
inv(3)	0 (0.0)	0 (0.0)	2 (0.5)	
t(1;22)	3 (6.6)	0 (0.0)	0 (0.0)	
t(7;12)	2 (4.4)	1 (1.7)	0 (0.0)	
Normal karyotype	6 (13.3)	6 (10.3)	68 (20.0)	
Others	13 (28.8)	31 (53.4)	82 (24.1)	
ND	1 (2.2)	0 (0.0)	2 (0.5)	
FLT3-ITD status				
Positive	0 (0.0)	3 (5.1)	44 (12.9)	0.002
Negative	44 (97.7)	55 (94.8)	296 (87.0)	
ND	1 (2.2)	0 (0.0)	0 (0.0)	

WBC white blood cell count, *FAB* French–American–British, *RAEB* refractory anemia with excess blasts, *RAEB-T* refractory anemia with excess blasts in transformation, *ND* not detected, *ITD* internal tandem duplications

[a] As the World Health Organization classification (3rd edition) was used, patients with <30 % bone marrow blasts were included in this study

The results of induction therapies are described in Table 2. The proportion of patients with <5 % bone marrow blasts following initial induction therapy and the complete remission (CR) rate were significantly worse in infants than in patients aged 1 to <2 years or in those aged ≥2 years, respectively. This was due to the higher early mortality rate in infants than in other age groups. CR could not be evaluated in two infants who discontinued the study because of an adverse event (patient #2 in Table 3) and at the physician's decision.

Of the 33 infants who achieved CR, 1 patient with inv(16) was included in the low-risk group, 26 in the IR group, and 5 in the HR group. Four patients in the HR group received allogeneic HSCT at the first CR (Fig. 2). One infant discontinued the study because of the physician's decision. When we compared the 3-year pEFS among the three age groups, pEFS was lower in infants (46.1 %, 95 % CI 31.1–59.9 %) than in those aged 1 to <2 years (55.4 %, 95 % CI 41.2–67.5 %) or those aged ≥2 years (55.2 %, 95 % CI 49.4–60.5 %). However, the

Table 2 Initial treatment response according to age group and before/after the protocol amendments

Age group	<1 year				1 to <2 years	≥2 years	*P* value[b]
	Before amendment $n = 28$	After amendment $n = 17$	*P* value[a]	Total $n = 45$	$n = 58$	$n = 340$	
<5 % bone marrow blast after Ind-1	16 (57.1 %)	12 (70.5 %)	0.367	28 (62.2 %)	51 (87.9 %)	290 (85.2 %)	0.001
CR rate (after Ind-2)	19 (67.9 %)	14 (82.4 %)	0.488	33 (73.3 %)	49 (84.4 %)	299 (87.9 %)	0.036
Early death (≤42 days)	5 (17.9 %)	0 (0.0 %)	0.140	5 (11.1 %)	1 (1.7 %)	1 (0.2 %)	<0.001
Non-response	2 (7.1 %)	3 (17.6 %)	0.350	5 (11.1 %)	6 (10.3 %)	32 (9.4 %)	0.922
Other	2 (7.0 %)	0 (0.0 %)	0.519	2 (4.4 %)	2 (3.4 %)	8 (2.3 %)	0.670

Ind-1 induction course 1, *CR* complete remission, *Ind-2* induction course 2

[a] Before versus after the protocol amendments

[b] Comparison among the three age groups

Table 3 Characteristics of the six infants who died during the initial induction phase

Patient	Characteristics at diagnosis					Cause of early death	Death (day+)	Infectious complications	Other complications
	Age (months)	Sex	WBC (/μL)	EMD	AML subtype (WHO-3/ FAB)				
#1	7	F	58,000	Yes	Acute monoblastic leukemia/M5a	Leukemia	5	No	No
#2	7	F	152,130	Yes	AML with 11q23 abnormalities/M5a	ARDS	62	Sepsis	HPS
#3	4	M	7,200	Yes	Acute monocytic leukemia/ M5b	ARDS	39	FN	HPS
#4	7	M	7,900	Yes	Acute monoblastic leukemia/M5a	ARDS	22	RSV infection	No
#5	7	M	7,840	Yes	AML with 11q23 abnormalities/M4	ARDS	39	RSV infection	HPS
#6	2	F	4,400	No	AML with multilineage dysplasia/M1	IP	17	Sepsis (*S. aureus*)	No

WBC white blood cell count, *EMD* extramedullary disease, *AML* acute myeloid leukemia, *WHO-3* World Health Organization (WHO) classification of tumors of hematopoietic and lymphoid tissues (3rd edition), *FAB* French–American–British, *F* female, *M* male, *ARDS* acute respiratory distress syndrome, *IP* interstitial pneumonia, *FN* febrile neutropenia, *RSV* respiratory syncytial virus, *S. aureus Staphylococcus aureus*, *HPS* hemophagocytic syndrome

difference was not statistically significant ($P = 0.108$) because of the relatively small numbers of patients (Fig. 3a). The median follow-up time of living patients was 3.06 years (range, 0.84–5.36 years). However, the 3-year pOS was significantly worse in infants (55.9 %, 95 % CI 37.9–70.6 %) than in those aged 1 to <2 years (77.0 %, 95 % CI 62.7–86.3 %) and those aged ≥2 years (74.7 %, 95 % CI 69.2–79.4 %; $P = 0.037$; Fig. 3b). The inferior survival rate in infants appeared to be due to the higher non-relapse mortality rate in this age group, rather than recurrent disease (Fig. 3c, d). The non-relapse mortality rates in infants, those aged 1 to <2 years, and those aged ≥2 years were 29.2 % (95 % CI 15.6–50.4 %), 7.4 % (95 % CI 2.8–18.9 %), and 11.8 % (95 % CI 8.3–16.7 %), respectively ($P = 0.007$). The cumulative relapse rates were 44.0 % (95 % CI 29.8–61.2 %), 41.0 % (95 % CI 29.0–55.8 %), and 42.6 % (95 % CI 37.3–48.3 %), respectively ($P = 0.564$).

Remission induction results of infants enrolled before and after the protocol amendments

We next compared the outcomes between 28 infants who were enrolled before the protocol amendments and 17 patients enrolled after these amendments. Before the protocol amendments, there were 5 early deaths plus 1 patient who died on day 62 during the initial induction phase (Table 3). These six deaths that occurred during initial